FINAL YEAR PROJECT

Physical Solubility of Carbon Dioxide in Decane ($C_{10}H_{22}$) Solvent from a CO_2/CH_4 System

By

Xolile Petunia Msimanga

Dissertation submitted in partial fulfillment of
the requirements for the
Bachelor of Engineering (Hons)
(Chemical Engineering)

MAY 2013

Universiti Teknologi PETRONAS
Bandar Seri Iskandar
31750 Tronoh
Perak Darul Ridzuan

CERTIFICATION OF APPROVAL

Physical Solubility of Carbon Dioxide in Decane ($C_{10}H_{22}$) Solvent from a CO_2/CH_4 System

by

Xolile Petunia Msimanga

A project dissertation submitted to the
Chemical Engineering Programme
Universiti Teknologi PETRONAS
in partial fulfillment of the requirement for the
BACHELOR OF ENGINEERING (Hons)
(CHEMICAL ENGINEERING)

Approved by,

_____

Dr. Nurhayati Bt. Mellon

UNIVERSITI TEKNOLOGI PETRONAS

TRONOH, PERAK

May, 2013

CERTIFICATION OF ORIGINALITY

This is to certify that I am responsible for the work submitted in this project, that the original work is my own except as specified in the references and acknowledgements, and that the original work contained herein have not been undertaken or done by unspecified sources or persons.

_____

XOLILE PETUNIA MSIMANGA

ACKNOWLEDGEMENTS

First and foremost, I would to express my thanks to God and my family for their love and support throughout the years. Secondly, my sincerest of gratitude to my Supervisor Dr. Nurhayati Bt. Mellon who in spite of her very busy schedule, found time to supervise and help me throughout the whole project period. Her support, attention and advice really helped the progression and completion of my project.

I would like to express my appreciation to the technicians working at the Unit operation lab in Block 3, especially Mr. Shahafizan, for their guidance, supervision and support provided within the course of the execution of the project. I want to thank the rest of the Laboratory Facilities Services Unit (LFSU) personnel as well for the support. I would also like to thank Mr. Shuaib, the PhD student who allowed me to part time on the equipment and also conducted my training for use of the experimental equipment. I am grateful that he took time out of his research to help me and my fellow course mate.

I want to thank Universiti Teknologi PETRONAS, more especially my department, my second residence in Malaysia, the Chemical Engineering department for giving me the opportunity to learn, network and develop my communication skills as well as to incorporate some of my theoretical knowledge with laboratory work as well as simulation studies through a compulsory course. Last, but not least, I want to thank everyone who directly or indirectly contributed to the completion of this work either through action or just through motivation, without them, I wouldn't have made it.

ABSTRACT

An investigation of the potential removal of Carbon Dioxide (CO_2) from a gas stream containing CO_2 and methane (CH_4) using n-decane ($C_{10}H_{22}$) as the physical solvent is presented. Physical absorption has been identified as one of the most effective ways to capture CO_2 from natural gas streams as it can handle high pressures and high concentrations of CO_2. The study is divided into two parts – the solubility experiment, and a simulation of the process in Aspen HYSYS. The solubility experiments were conducted to predict the solubility of CO_2/CH_4 at different temperatures and pressures using a high pressure gas solubility cell. The simulation was carried out at different pressures up to 60 bar, for various gas compositions. Two thermodynamic models were selected and analyzed, the PR-EOS and the SRK-EOS. Subsequently, the data obtained was used to estimate Henry's constant for CO_2. The simulation results for n-decane showed an increase in CO_2 capturing capacity at lower temperatures and at higher pressures, which is in agreement with Henry's law, and the absorption capacity was found to be selectively higher for CO_2 than for CH_4. Based on the experiment results; there was more absorption of CO_2 and CH_4 at lower temperatures and at a higher pressure, and that the absorption was selectively higher for CO_2 than it was for CH_4. Therefore, the simulation and the solubility experiment findings show that n-decane is a potential candidate as a physical solvent for the application of the removal of CO_2 from natural gas.

TABLE OF CONTENTS

LIST OF FIGURES

LIST OF TABLES

CHAPTER 1

INTRODUCTION

The investigation of gas solubility in liquids is important for the design of gas absorption processes to purify industrial and natural gases which often contain large quantities of carbon dioxide (CO_2) (Karim et al., 2010). Natural gas reservoirs are generally available at high partial pressures as well as high CO_2 concentrations (Keskes et al., 2006); this is prominent in South East Asian regions. This poses a challenge as most of the available CO_2 removal technologies cater for lower partial pressure and low CO_2 content streams. Physical absorption is often favored for treating gas streams at high partial pressures with high concentrations of acid gases (Murrieta-Guevara et al., 1988). At low partial pressures, physical solvents are unrealistic since the compression of the gas for physical absorption is costly (Burr & Lyddon, 2008). However, if the gas is available at high partial pressure, physical solvents are a better choice than chemical solvents (Karim et al., 2010).

1.1 Project Background

The most disturbing global environmental issues of today are the rise of global temperatures and the climate changes. These issues are mainly caused by the increasing atmospheric CO_2 concentration. Approximately 69% of carbon dioxide (CO_2) emissions and 60% of greenhouse gas emissions are energy-related (Tan et al, 2011). Natural gas has become one of the main energy sources. It is used primarily for generating steam for electric power, producing heat, and as fuel for vehicles (Gupta et al, 2003). Currently, there is a lot of interest in natural gas

exploration as natural gas provides a cleaner and less environmentally harmful fuel supply than other conventional fossil fuels (Arronwilas & Vaewab, 2007).

The increasing importance of natural gas as a source of energy due to its efficiency, and as an environmentally cleaner fuel supply, poses difficult gas separation design challenges, as the streams recovered from gas fields are at high pressures and can contain a high fraction of CO_2 (Keskes et al., 2011) and most current technology is designed for lower pressures and low concentrations of CO_2. There are several routes of CO_2 removal such as; solid adsorption, absorption into a liquid solvent, membranes or other physical and biological separation methods (Kohl & Nielsen, 2005). This research focuses on using physical absorption as the method of separation since it can operate at high partial pressures and concentrations of CO_2.

Higher chain alkanes have been established as a possible alternative for the removal of CO_2 from natural gas based on a study done by Ryan-Holmes using CO_2/CH_4 in butane; the study showed that CO_2 was preferentially absorbed (GPSA, 2004). This is the reason for selection of n-decane as a possible physical solvent for CO_2 removal. Today, computer-aided process simulation is nearly universally recognized as an essential tool in the process industries. Therefore the simulation portion of the investigation was undertaken to verify the suitability of the application of HYSYS simulators' thermodynamic models in the prediction and correlation of the solubility of CO_2/CH_4 in a decane physical solvent at various pressures and different temperatures.

This project will present a review of different processes available and suitable for removal of CO_2 from natural gas. In this project the physical solubility of CO_2 in decane from a CO_2/CH_4 system will be investigated at (308.15 and 318.15, and 328.15) K and (10 and 30) bar, temperature and pressure, respectively for the high pressure solubility experiment. For the simulation the CO_2/CH_4 system will be investigated at (308.15 and 318.15, and 328.15) K and at pressures up to 60 bar and

at varying compositions of CO_2 and CH_4. The selection of the temperature and pressure range is based on offshore processing conditions at which natural gas is retrieved from the gas fields and CO_2 physical properties.

1.2 Problem Statement

CO_2 can be found in significant quantities in natural gas streams at high partial pressures and concentrations. Conventional separation techniques are usually restricted to low CO_2 content and/or low-pressure feeds (Pereira et al, 2011). Therefore, there is a pressing need for an alternative process that is appropriate for CO_2 rich natural gas streams. Physical absorption is ideal as it favours high partial pressures of CO_2. There are various physical solvents that are available, but are not favourable due to harmful environmental effects and costly operations. (Keskes et al, 2006).

The literature survey indicates that there is limited information available on the effect of dissolved CO_2 on the properties of pure hydrocarbons physical solvents and minimal data for the ternary system of CO_2 + methane + decane has been reported (Kariznovi et al. 2013). In this study, the main aim is to develop an understanding of the solubility of CO_2 from a CO_2/CH_4 system in a decane solvent. The measurements that will be presented will determine the liquid phase composition and the gas loading when a liquid hydrocarbon solvent (*n*-decane) is saturated with CO_2 and methane.

1.3 Objective

The objective of this research investigation is to provide the experimental data of a CO_2/CH_4 system and to assess the physical solubility of CO_2 in the n-alkane solvent, decane.

1.4 Scope of work

The scope of work for this project:

- Conduct an extensive literature research on the solubility and equilibrium data for CO_2/hydrocarbon systems.
- Model the base case process in the Aspen HYSYS at various concentrations, temperatures and pressures.
- Experiment and evaluation using the same operating conditions as Aspen HYSYS simulation for CO_2 and for CH_4 – High Pressure Solubility Cell.
- Comparison of the results obtained from the experiment to the predicted Aspen HYSYS results. Evaluation of competitive removal of CO_2/CH_4 in decane.

1.5 Feasibility of the project

The period given for completion of the research project was two semesters which comprised of 28 weeks. The chemicals and the apparatus for the solubility experiment were all available in the Unit Operations lab in Block 3, Chemical Engineering Department, Universiti Teknologi PETRONAS. Based on all of this information it was feasible that the project could be completed in the stipulated time.

CHAPTER 2

LITERATURE REVIEW

2.1 INTRODUCTION

Carbon dioxide (CO_2) is an important non-hydrocarbon component in chemical engineering and the petroleum industry due to its characteristics. CO_2 is a naturally occurring gas that is 50% heavier than air, is colourless and odourless. It has low critical point and is cheap and non-toxic (Nourozieh et al., 2013). The increase in demand for energy worldwide has aided the search for alternative sources of primary energy. The major alternative source with less environmental impact that has been discovered is energy obtained from natural gas. Some deposits of natural gas at geological conditions contain contaminants such as CO_2 and H_2S, which constitute great environmental hazards when they get to the atmosphere and also hinder natural gas processes (www.standord.edu, 2005).

According to the definition given by the United States Environmental Protection Agency (EPA), CO_2 capture and sequestration (CCS) is a set of technologies that can greatly reduce CO_2 emissions from new and existing coal- and gas-fired power plants and large industrial sources. When there is an excessive amount of greenhouse gases – more heat is trapped within the earths' atmosphere, and this leads to an increase in global warming. CO_2 is one of these greenhouse gases – therefore certain measures, such as CO_2 capture, have been put into place to decrease the emissions, thus slowing down global warming.

Gas treating or sweetening are both terms used to describe the various processes for removal of certain contaminants; primarily hydrogen sulphide (H_2S) and CO_2, from natural gas or hydrocarbon liquids.There is a lot of interest in developing methods to remove CO_2 from natural gas streams. The increasing importance of natural gas as a source of energy due to its efficiency, and as an environmentally clean fuel supply, poses difficult gas separation design challenges, as the streams recovered from gas fields are at high pressures and can contain a high fraction of CO_2 (Keskes et al., 2011) and most current technology is designed for lower pressures and low concentrations of CO_2.

2.2 CO_2 REMOVAL PROCESSES

The main objective of CO_2 capture is to produce a stream of CO_2 which can be transported and put underground or in deep oceans. CO_2 capture is not really a new theory to industry, the capture processes have been widely applied in the natural gas processing chemical industry for over 60 years and current practice is simply just to vent it to into the atmosphere. **FIGURE 2.1** below gives an idea about CO_2 capture routes in a broad range of fossil energy conversion processes (Gupta et al. 2003).

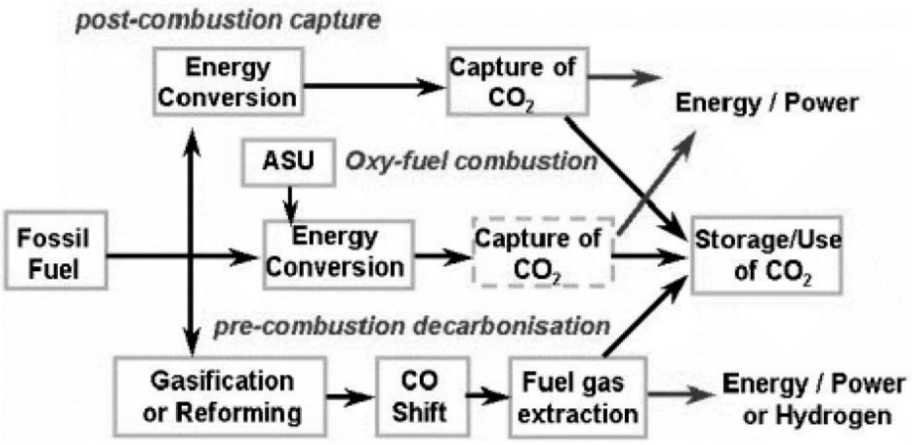

FIGURE 2.1: CO_2 capture pathways in fossil energy conversion processes (Gupta et al. 2003)

Varieties of processes have been developed over the years to treat certain types of gases with the aim of optimizing capital cost and operating cost, meet gas specifications and for environmental purposes. **FIGURE 2.2** below outlines the various technologies available for CO_2 Capture.

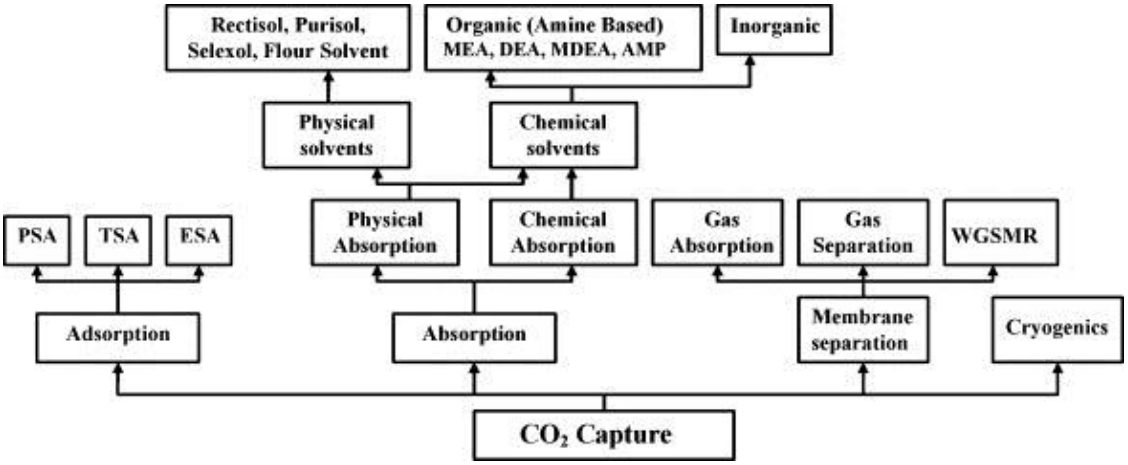

FIGURE 2.2: Carbon Capture technologies (Padurean et al. 2011)

The selection of a technology for a given capture application depends on various factors i.e partial pressure of CO_2 in the gas stream, extent of CO_2 recovery required, sensitivity to impurities, purity of desired product, capital and operating costs of the process (White et al, 2003).

2.2.1 Chemical absorption process

Chemical absorption processes are based on the exothermic reaction of the solvent with the gas stream to remove the CO_2 present in the stream (Georgiadis & Pistikopoulos, 2008). In chemical absorption, the solvent loading assumes a non-linear dependence on the partial pressure and is higher at lower partial pressures. Large increases in the partial pressure of the gas results in a very small increase in the solvent loading (Gupta et al, 2003). In chemical absorption, heating or reboiling is necessary for solvent regeneration which leads to high capital costs.

2.2.2 Membrane process

A membrane is a barrier film that allows selective and specific permeation under conditions appropriate to its function (Georgiadis & Pistikopoulos, 2008). Gas separation membranes rely on differences in physical or chemical interactions between gases and a membrane material, causing one material to pass through faster than another. Membrane technology has not yet been optimized for large volume of gas separation. Membranes cannot usually achieve high degrees of separation, so multiple stages and/or recycle of one of them is necessary. This leads to increase complexity, energy consumption and costs. (Gupta et al, 2003)

2.2.3 Adsorption process

This process involves the absorption of acid gas components by a solid adsorbent. The intermolecular forces between the CO_2 and the surface of the solid material permit separation by adsorption. The removal processes is either by chemical reaction or by ionic bonding of solid particles with the acid gas. Selective adsorption of the gases depends on temperature, partial pressures, surface forces and adsorbent pore size (Georgiadis & Pistikopoulos, 2008). Adsorption is not yet considered attractive for large scale separation of CO_2 because the capacity and CO_2 selectivity of available adsorbents is low. (Gupta et al, 2003)

2.2.4 Cryogenic process

This is a commercial process commonly used to liquefy and purify CO_2 from relatively high purity (>90%) sources. The gases are cooled to a very low temperature (lower than -73.3^{o}C) in order to freeze-out the CO_2 and separate it (Georgiadis & Pistikopoulos, 2008). Since CO_2 has a high triple point, 216.58 K, formation of solid phase in the stream is unavoidable. The presence of a solid phase in cryogenic processing produces major problems such as blockage of process equipment, plant shut-downs, and other safety hazards. It makes useful natural gas

sources uneconomical (www.standord.edu, 2005). Furthermore, cryogenic processing is economically unattractive as refrigeration leads to high capital costs.

TABLE 2.1: Advantages and disadvantages of carbon capture processes

Carbon Capture Process	Advantage	Disadvantage
Physical Absorption	• No absorption limitation • Ideal for high pressure and concentration of CO_2	• Possibility of co-absorption of hydrocarbons if concentration of heavy hydrocarbons is high
Chemical Absorption	• Ideal for removal of CO_2 at low concentrations (3%-25%)	For CO_2 rich gas streams: • Costly to regenerate solvent • Limited by stoichiometry of chemical reaction. • High energy requirements
Adsorption	• Ideal for purification - CO_2 decrease typically from 3% to 0.5%	• For CO_2 rich streams constant regeneration of solid bed will be required
Membrane Separation	• Can be adjusted to changes in CO_2 content	• Natural gas contaminants may lead to deterioration, thus decreasing reliability, and regular replacement of the membrane
Cryogenic Separation	• CO_2 can be obtained at relatively high pressure.	• Large refrigeration requirement - utilizing more power

Sources: [1] Georgiadis & Pistikopoulos, (2008)
[2] Stanford University – GPEC
[3] GPSA, 2004

2.3 Physical absorption processes

Physical solvent processes use organic solvents to physically absorb CO_2. The removal of CO_2 is based on the solubility of CO_2 within the solvents. The solubility of CO_2 depends on the partial pressure and temperature of the feed gas. The amount of CO_2 absorbed by the solvent is determined by the vapour-liquid equilibrium of the mixture, which is governed by the pressure and temperature (Georgiadis & Pistikopoulos, 2008). At high CO_2 partial pressure, the CO_2 loading capacity of the solvent has the potential to be high for a physical solvent. Hence, physical absorption processes are particularly appropriate for the treatment of high pressure CO_2-rich natural gas streams. (Pereira et al, 2011)

According to (GPSA, 2004), in general, a physical solvent process should be considered when:

- The partial pressure of the acid gas, namely CO_2, in the feed is greater than 345 kPa.
- The heavy hydrocarbon concentration in the feed gas is low.
- Bulk removal of the acid gas is desired.
- Selective removal of CO_2 is desired.

There are various physical solvent processes for the removal of CO_2 from natural gas streams, but not all the processes available are capable of removing CO_2 for industry specifications of 50- 100 ppmv or 2.5% of CO_2 in the product stream (GPSA, 2004). There are various physical solvents used commercially today for the absorption of CO_2 and other acid gases from natural gas streams. These are namely; the Selexol process, Rectisol process and the Fluor process. This is a brief description of each and **TABLE 2.2** outlines the advantages and disadvantages of each.

2.3.1 Selexol Process

This process uses a polyethylene glycol derivative as a solvent. The solvent is selective for RSH, CS_2, H_2S, and other sulfur compounds. The process can be used to selectively or simultaneously remove sulfur compounds, carbon dioxide, water, as well as paraffinic, olefinic, aromatic and chlorinated hydrocarbons from a gas or air stream (GPSA, 2004).

2.3.2 Rectisol Process

This process uses methanol as a solvent, and was developed by the German Lurgi Company and Linde A. G. Because of the vapor pressure of methanol, the process is normally applied at temperatures of –35°C to –73°C for the Rectisol

solution. The process is best suited where there are limited quantities of ethane and heavier components (GPSA, 2004).

2.3.3 Fluor Solvent

This process patented by the Fluor Corporation, is based on the use of anhydrous propylene carbonate. The temperature of the lean solution to the absorber is usually well below ambient, and some method of refrigerating the solvent is usually necessary (GPSA, 2004).

TABLE 2.2: Advantages and disadvantages of various physical solvents

Physical Solvent	Advantage	Disadvantage
Selexol - Dimethyl ethers of polyethylene glycol	• Glycol is effective for capturing both CO_2 and H_2S at higher concentration • Lower energy demand	• CO_2 is released at near atmospheric pressure - requiring recompression. • The solvent have high affinity to heavy hydrocarbon which will be removed with CO_2 and essentially result to hydrocarbon losses.
Rectisol - Methanol	• Reduced solvent flow rate for CO_2 removal • Non-corrosive • Have high thermal and chemical stability.	• The complex scheme and the need to refrigerate the solvent result in high capital and operating cost of the plant - most costly process for treating acid gas
Flour - Propylene carbonate	• High CO_2 solubility and enhance CO_2 loading • The operation is simple and a dry gas as output product.	• Requires little or no H_2S • The FLUOR solvent is very expensive • The solvent have high affinity to heavy hydrocarbon which will be removed with CO_2 and essentially results to hydrocarbon losses.

(Source: GPSA, 2004)

2.4 Separation of CO_2 and Methane

2.4.1 Choice of solvent

Like n-butane, other alkanes such as n-decane are known to absorb CO_2 preferentially to CH_4. Experimental findings indicate K-values [separation factor, K = (CO_2:CH_4)liquid / (CO_2:CH_4)gas] ranging from 1.2 to 1.8 (Dunyushkin et al., 1977). The alkane solvent presents the advantage of being cheap, easily available

and tuneable (mixture of alkanes) (Georgiadis & Pistikopoulos, 2008). Thus, there is now interest in investigating heavier alkanes with similarly higher boiling points to see if it is possible to conduct the separation under non-cryogenic conditions and still have the same satisfactory CO_2/CH_4 separation (GPSA, 2004).

Longer *n*-alkanes are likely to be too viscous while shorter *n*-alkanes are likely to be too volatile for the temperature range of interest. (Pereira et al, 2011). Therefore, the task now is to find the optimal hydrocarbon or mix of hydrocarbons that will provide the best separation at the desired operating conditions for offshore processing. For the purpose of this investigation the straight chain alkane – decane will be the solvent to see its suitability as a solvent for this process.

2.4.2 Ryan-Holmes Cryogenic Separation

According to GPSA (2004) extractive distillation under cryogenic conditions can be used as a method for the separation of CO_2 from methane. This was an approach developed by Ryan-Holmes – and it involved the addition of a third heavier hydrocarbon to the CO_2/CH_4 system. The addition of the third stream – which could be any hydrocarbon heavier than CH_4, significantly alters the solubility characteristics of the system to the point where almost any purity of methane can be produced. For their investigation Ryan-Holmes used n-butane as their n-alkane component and it was found that with the addition of the n-butane, the separation could be carried through without CO_2 solid formation. Adding greater amounts of the additive increased the safety margin away from the CO_2 solid formation region.

FIGURE 2.3 shows the effect of adding the third component (n-butane) to a CO_2/CH_4 distillation column. By adding n-butane, a column operation profile without CO_2 solid formation can be achieved. Adding greater amounts of the additive increases the safety margin away from the CO_2 solid formation region.

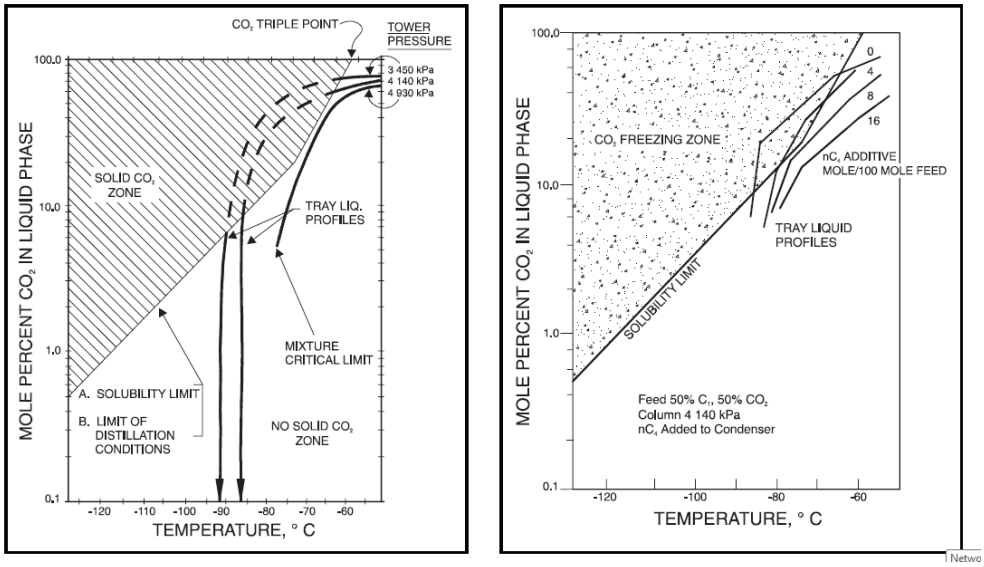

FIGURE 2.3 – Distillation Profile CH_4-CO_2 Binary and Distillation Profile Binary Feed with nC_4 Additive (GPSA, 2004)

2.5 Solubility of gases

Solubility is defined as the ability of a substance to dissolve in another substance. In a process of dissolving, the substance which is being dissolved is called the solute while the substance in which the solute is dissolved is called the solvent (Helmenstine). Solubility of a gas in a liquid depends on the temperature, partial pressure of the gas over the liquid, as well as nature of the solvent and the gas. Gas solubility is always limited to the equilibrium between the gas and the saturated solution of the gas. The dissolved gas will always follow Henry's law (Trefil, 2003).

In general, the solubility of gases decreases with increasing temperature. The decrease in gas solubility as temperature increases is primarily a function of kinetic energy - as temperature increases, the kinetic energy of dissolved gas will increase, making it easier for the gas molecules to escape the solution. Inversely, solubility of a gas increases with increasing pressure. If the pressure of a gas increases under isothermal conditions, more gas molecules are striking the surface of the container in a given amount of time (Ebbing & Gammon, 2010). A gas in contact with a solution is "dissolved" when gas molecules strike the surface of the solution. Thus, increasing

the pressure isothermally results in more collisions of the gas molecules, per unit time, with the surface of the solvent; this results in greater solubility.

The concentration of the dissolved gas depends on the partial pressure of the gas. The partial pressure controls the number of gas molecule collisions with the surface of the solution. If the partial pressure is doubled, the number of collisions with the surface wall will also double. Increased number of collisions would produce more dissolved gas (Reger et al., 2009). The illustration of the phenomena is shown in **FIGURE2.4** below.

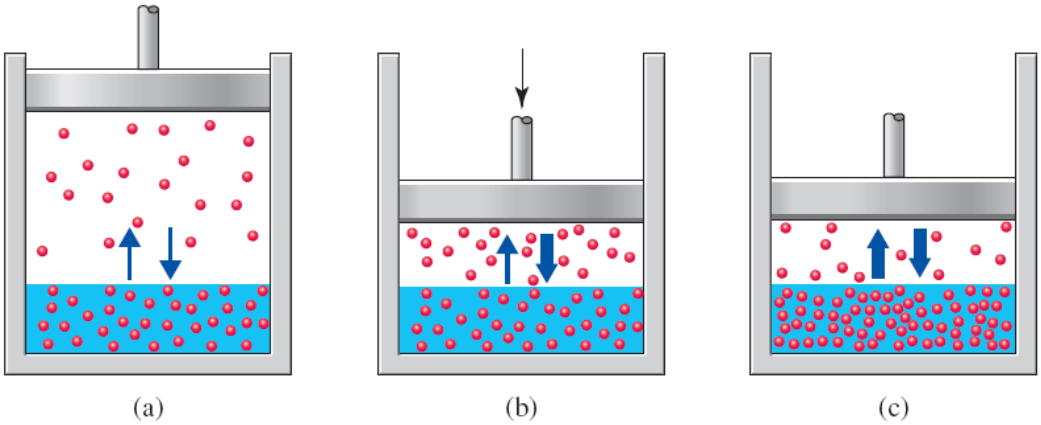

FIGURE 2.4: Solubility of a Gas Depends on Its Partial Pressure above the Solution

The number of gas molecules leaving the gas phase to enter the solution equals to the number of gas molecules leaving the solution. If the temperature remains constant, increasing the pressure will increase the amount of dissolved gas.

2.6 Equilibrium data of CO_2/Hydrocarbon systems

Physical solubility data of CO_2 gas is required to predict the gas absorption rate. The measurement of physical solubility is based on determining the concentration of gas absorbed in a solvent at equilibrium. The vapour–liquid equilibrium (VLE) data of binary mixtures CO_2 and *n*-alkane have been extensively considered in literature. This is a brief overview of a study conducted by (Kariznovi et al, 2013) on the history of systems involving CO_2 and decane. In 1963, Reamer

and Sage reported the experimental measurements of the volumetric and phase behaviour of CO_2 and *n*-decane binary system at pressures up to 69 MPa and temperatures between 277.6 K and 510.9 K. Then in 1974 Kulkarni *et al.*, studied the same system and obtained the pressure, composition, and molar volume data of the two co-existing liquid phases as a function of temperature along the three-phase (liquid, liquid and vapor) curve. Wilcock *et al.* determined the solubilities of CO_2 in *n*-octane and *n*-decane at atmospheric pressure in the temperature range 293K to 311 K.

In 1986, Nagarajan and Robinson did experiments to measure phase compositions and densities, and interfacial tensions for VLE of CO_2 and *n*-decane system at 344.3K and 377.6 K, and pressures up to the critical point. In 1997, Ashcroft and Isa measured the density of saturated hydrocarbons. They evaluated the effect of several dissolved gases, including CO_2, on the densities of liquid hydrocarbons. Their data showed that the saturation of hydrocarbon liquids with all gases results in the decrease of density while the density of saturated liquid increases for CO_2.

In 2001, Shaver *et al.* reported VLE of binary system CO_2 and *n*-decane at temperature 344.3 K. They measured the phase compositions, phase densities, and interfacial tensions. Tsuji *et al.* measured the bubble point pressure and liquid density data for CO_2 and decane system at 344.3 K. In 2006, Jiménez-Gallegos *et al.* measured the vapor and liquid equilibria for systems CO_2 + octane and CO_2 + decane from 322-372 K and 319-372 K, respectively. Ren and Scurto developed an experimental apparatus for determining high-pressure; vapour-liquid, liquid-liquid, solid-liquid-vapor, vapor-liquid-liquid equilibrium, and the mixture critical points and transitions. The authors reported the solubility as well as liquid density for (CO_2 and *n*-decane) system. **TABLE 2.3** is a summary on the studies done on properties of CO_2 physical solubility in decane and other similar solvents.

TABLE 2.3: Summary of previous research

Year	Reference	Pure light component	Heavy hydrocarbon(s)	*T*(K)	*P* (bar)	Data
1974	Kukarni et al.	Carbon dioxide	Decane	217–298	Up to 16.55	Phase composition and liquid molar volume
1986	Nagarajan and Robinson	Carbon dioxide	Decane	344–378	Up to critical point	Phase composition, phase density
1994	Iwai et al.	Carbon dioxide	Decane	311 and 344	44.8–113.7	Phase composition
2001	Shaver et al.	Carbon dioxide	Decane	344	Up to 126.6	Phase composition, phase density
2006	Jimenez-Gallegos et al.	Carbon dioxide	Octane and decane	319–372	19.5–155.8	Phase compositions
2006	Ren and Scurto	Carbon dioxide	Decane	344	16.55–98.4	Solubility and liquid density

Source: Kariznovi, Nourizieh, & Abedi, 2013

The literature survey indicates that there is limited information available on the effect of dissolved CO_2 on the properties of pure hydrocarbons and no data for the ternary system CO_2 + methane + decane systems has been thoroughly reported. In this study, the main aim is to develop an understanding of the solubility of CO_2 from a CO_2/CH_4 system in decane solvent. The measurements that will be presented at the end of this investigation will determine the equilibrium properties, liquid phase composition when a liquid hydrocarbon solvent (*n*-decane) is saturated with CO_2 and methane.

2.6 HYSYS Process Simulation Package

Aspen HYSYS is powerful software for steady and dynamic state simulation processes. The built-in property packages in HYSYS provide accurate thermodynamic, physical and transport property predictions for hydrocarbon, non-hydrocarbon, petrochemical and chemical fluids. The database consists of an excess of 1500 components and over 16000 fitted binary coefficients (HYSYS 7.2 User's Guide, 2011). It includes tools for estimation of physical properties and liquid-vapour phase equilibrium, heat and material balances, design, optimization of oil and gas processes and process equipment. HYSYS is an interactive and flexible process

operational improvement and asset management. Therefore enhance productivity, reliability, decision making and profitability of the plant life cycle.

2.6.1 Fluid Packages and Thermodynamic model selection

In HYSYS, all necessary information pertaining to pure components physical properties calculations is contained in the fluid package, choosing the right fluid package for a given component is vital (Karim et al., 2010). Proper selection of thermodynamic models during process simulation is also absolutely necessary as a starting point for accurate process modeling. A process that is otherwise fully optimized in terms of equipment selection, configuration, and operation can be rendered worthless if the process simulation is based on inaccurate fluid package and thermodynamics models.

Vapor-liquid equilibrium (VLE) relationships are needed in the solution of many engineering problems. The required data can be found by experiment, but such measurements are seldom easy, even for binary systems, and they become rapidly more difficult as the number of constituent species increases. This is the incentive for application of thermodynamics to the calculation of phase-equilibrium relationships.

For simulated processes involving hydrocarbons – the most reliable fluid packages are the Peng-Robinson equation of state (PR-EOS) and the Soave-Redlich Kwong equation of state (SRK-EOS) (Aspen Tech 2003). They normally use three pure-component parameters per substance. Thus, in the present work, SRK-EOS and PR-EOS were chosen.

Once the fluid package and the thermodynamics model equation are selected, it is now possible to enter the simulation environment where the detailed process

flow diagram of a given plant can be constructed. Simulation of the built process flow diagram is achieved by supplying important physical, thermodynamics and transport data of the stream and equipment involves, this is done until all the units and the streams are solved and converge. HYSYS require minimal input data from the user, the most important input parameters needed for streams to solve are the temperature, pressure and flow rate of the stream. HYSYS offers an assortment of utilities which can be attached to process stream and unit operations. The tools interact with the process and provide additional information. Once the HYSYS simulation is done the experimental portion of the investigation can be conducted and the results can be compared and the accuracy of HYSYS as well as the experimental calculations can be discussed.

CHAPTER 3

METHODOLOGY

3.1. Research Methodology and Project Activities

The methodology for conducting this research project is exploration and discovery. As this project is mainly an experimental research, the results obtained from this research can be used to compare with other literature results. Since the results obtained from this research will use a different configuration and setup of equipment - the equilibrium solubility process to remove CO_2 from CO_2-CH_4 binary system can be used as a basis of comparison with other research that has been done.

The results can hence further enhance the research and development of solubility processes for the removal of CO_2 from natural gas streams. The project activities in this research are mainly experimental work with basis on simulation. After a thorough literature review was done and the process was simulated in the desired software, experimental work was done to conduct the investigation.

3.2. Experimental Procedures/Approach

The following diagram illustrated by **FIGURE 3.1** shows the general experimental procedures that will be implemented in this research project.

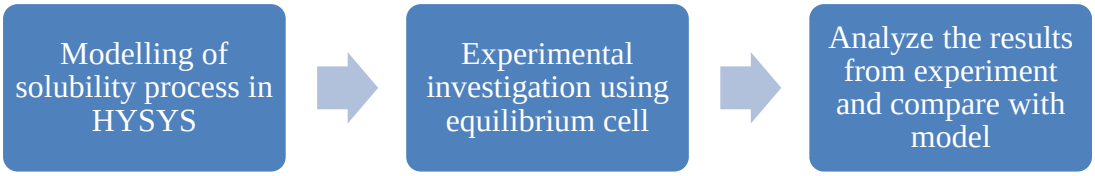

FIGURE 3.1: The schematic diagram depicting the general approach in this project

3.2.1. HYSYS Simulation Procedure

A base case was established using the following steps; the first step is to select the appropriate fluid package; as previously stated PR-EOS and SRK-EOS fluid selected as is shown in **FIGURE 3.2** below;

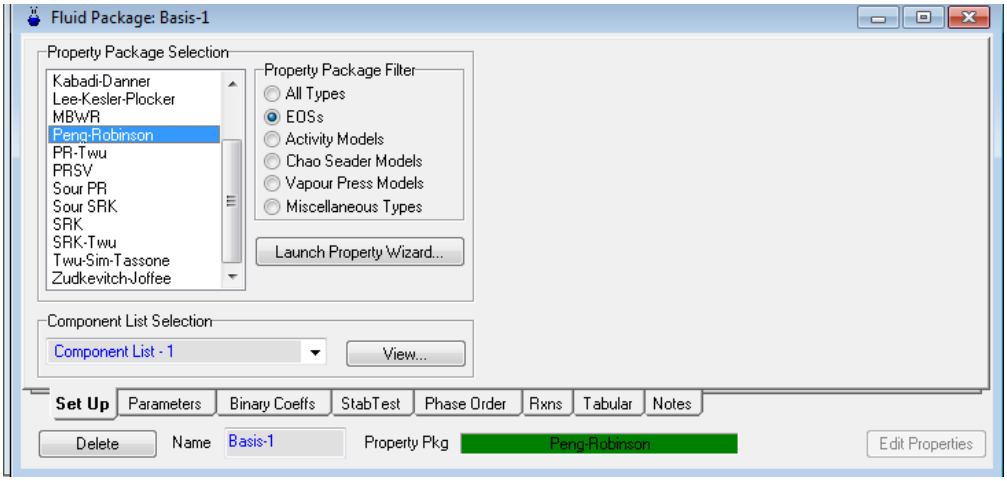

FIGURE 3.2: Fluid Package Basis

Next is the selection of components that will be involved in the simulation – in this case that is CO_2, CH_4 and n-Decane. The component selection window is opened by selecting view in the component-list show in **FIGURE 3.2. FIGURE 3.3** shows the dialog window used for the component selection.

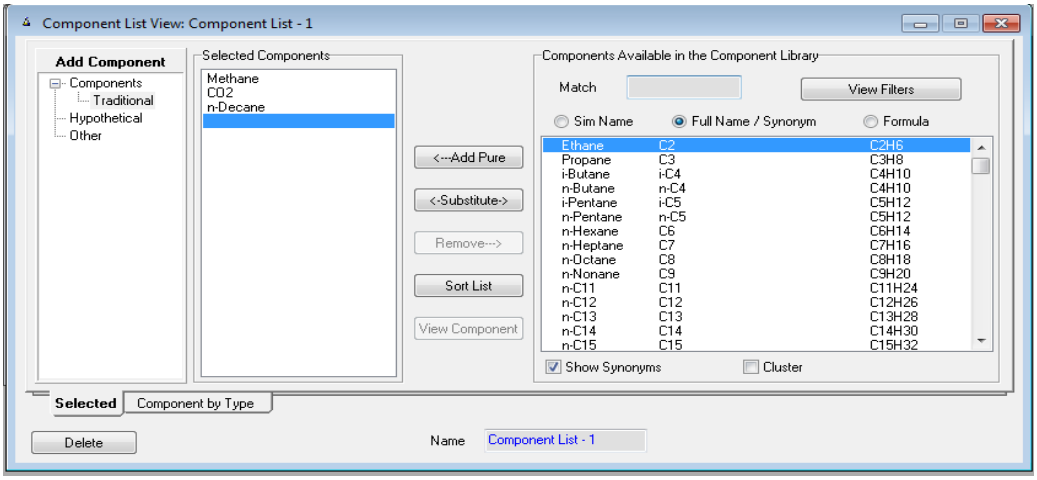

FIGURE 3.3: Component selection window.

After selecting the components, enter the simulation environment where the process simulation is done. For this simulation the selected components involved were very simple:

- CO_2/CH_4 feed stream (different compositions)
- Pure n-Decane stream
- Separator
- Energy stream (to create isothermal conditions required to mimic the experiment)
- Liquid product stream
- Gas product stream

FIGURE 3.4 illustrates how these were put together in the HYSYS simulator environment.

The simulation of the process begins with the simulation of the feed streams by specifying the gas/liquid temperature, pressure and flow rate and HYSYS calculates the remaining parameters. The heat duty to be provided by the energy stream (red stream) is entered by the user in order to make the process isothermal by either adding or removing heat to the separator.

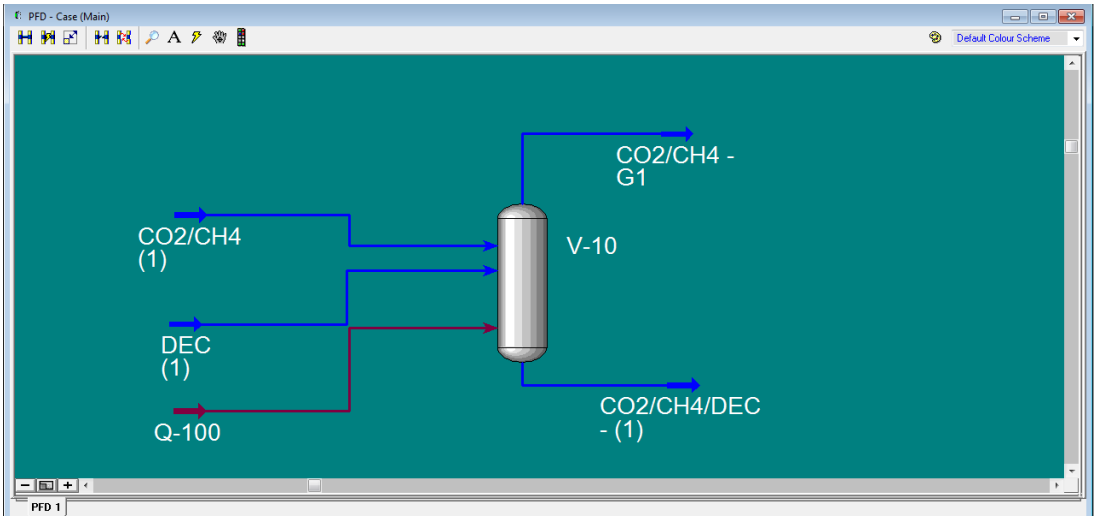

FIGURE 3.4: Simulated process for solubility

HYSYS then generates a worksheet that shows the operating conditions for each stream as well as the composition. **FIGURE 3.5** shows the composition window which is where the results for this part of the investigation were obtained.

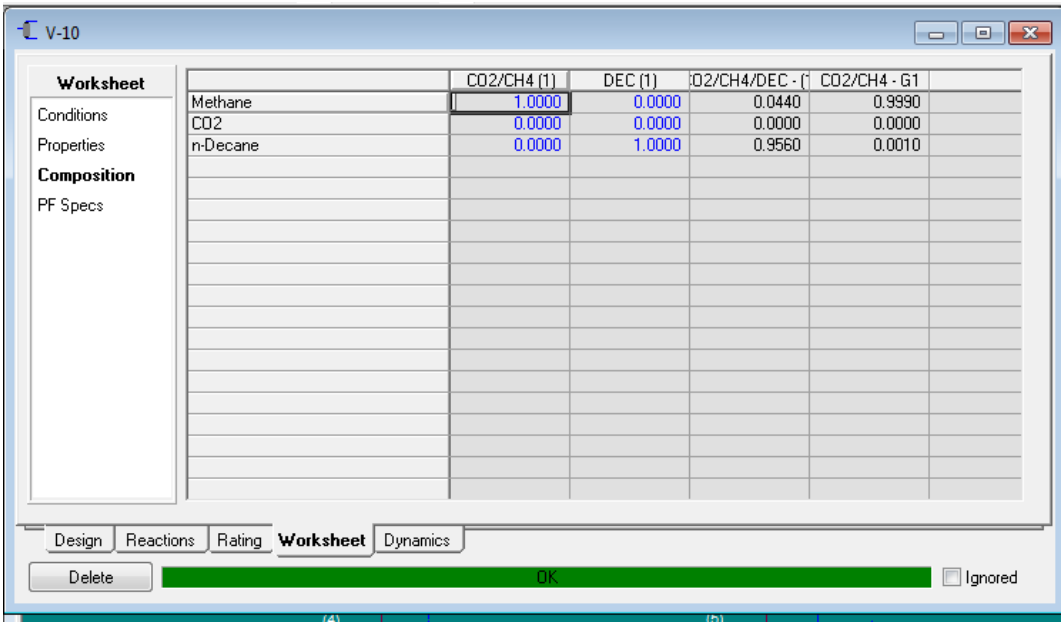

FIGURE 3.5: Window showing composition of each stream.

The green bar at the bottom of the window is to indicate that the simulation was successful and that the values converged.

3.2.2. Solubility Experiment Equipment

Materials and equipment

The materials involved in this experiment are listed as the following:

i. Carbon Dioxide (gas) - 99.8% purity purchased from Malaysian Oxygen Berhad
ii. Methane (gas) - 99.5% purity which is purchased from Mox-Linde gases Sdn. Bhd
iii. n-Decane solvent - liquid form at 99% purity and it was purchased from Sigma-Aldrich Inc.

The equipment used for this experiment is as listed below:

i. Two (2) pressure cells; mixing vessel and an equilibrium cell
ii. Compressor
iii. Magnetic stirrer
iv. Metering pump
v. Water bath

In compliance to the safety requirements of the laboratory regulations, the following are worn throughout the experiments:

i. Lab coat
ii. Covered shoes
iii. Gloves
iv. Safety goggles

Description

Two pressure vessels are mainly used in this experiment in which one is the mixing vessel (MV); to store the CO_2/CH_4 gas, and the other one is the equilibrium cell (EC); where the gas and solvent are mixed. Both of the vessels are thermo regulated with water bath set at the required temperatures. In order to elevate the pressure, a compressor is used. After the parameters are set, the basic experimental

procedures, pressure reading taking and sample taking are repeated for temperatures and pressures ranging at (308.15, 318.15 and 328.15) K and (10 and 30) bar, respectively.

Basic Procedure:

Solvent is transferred to EC

Gas is transferred from MV to EC

Wait until equilibrium is achieved

The following pressure readings are taken for data analysis:

i. P_1, the initial pressure of MV.
ii. P_2, the stabilized pressure of MV and EC when gas is transferred.
iii. P_{eqm}, the equilibrium pressure of EC.

High Pressure Gas Solubility Cell

The solubility measurement for this research project was conducted using the SOLTEQ High Pressure Gas Solubility Cell (Model: BP22). The unit is capable of operating up to a pressure of 65 bar and the temperatures can be maximised to 300^{o}C. The location of the unit is in the Unit Operations Lab, Block 3, Universiti Teknologi PETRONAS.

FIGURE 3.6 shows the solubility apparatus used while the schematic diagram of the experimental setup to determine the physical solubility of CO_2 is shown in **FIGURE 3.7.**

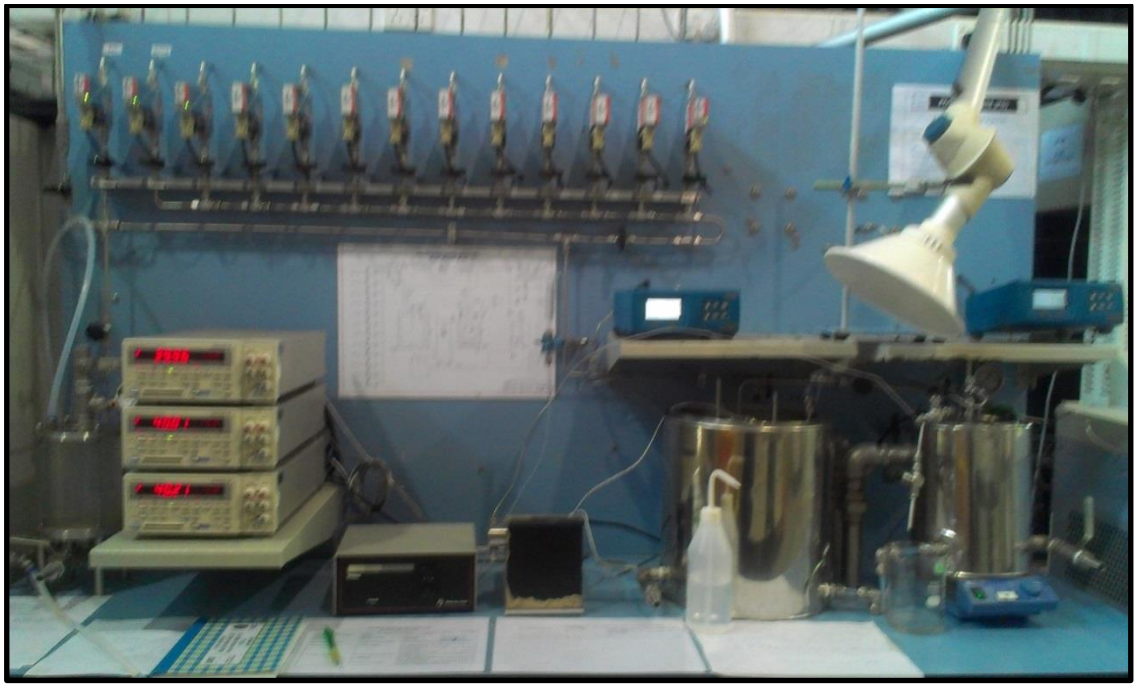

FIGURE 3.6: High Pressure Gas Solubility Cell

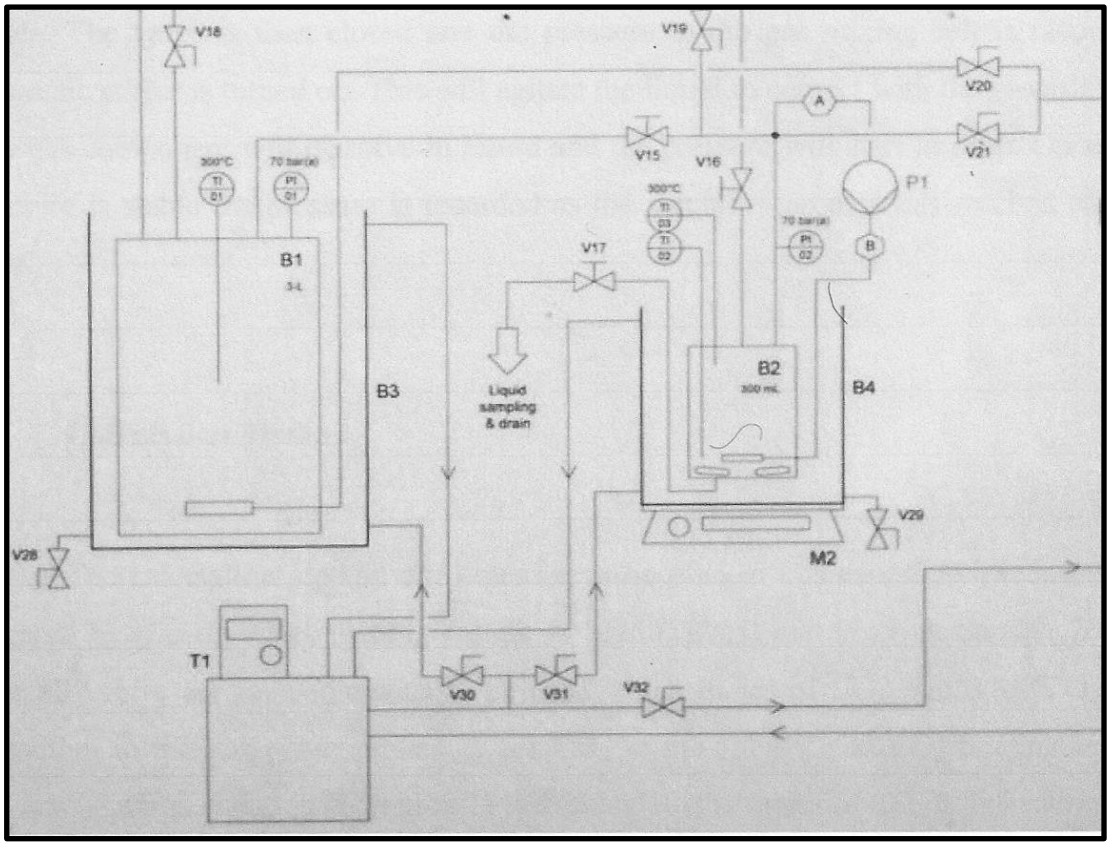

FIGURE 3.7: Schematic Diagram of High Pressure gas solubility cell

The SOLTEQ High Pressure Gas Solubility Cell consists of a stainless steel mixing vessel with a volume of 3L and a 50mL equilibrium cell. Both are immersed in stainless steel containers with bottom and side insulation, with tangential inlet and outlet ports for the thermostat connections heating jacket. Other supporting components include the magnetic stirrer, circulation pumps, vacuum pump, thermostat heating bath, liquid feed pump, liquid degassing unit and instrumentation such as; the mass flow controllers, and the pressure and temperature indicators. Both the mixing vessel and the equilibrium cell are immersed in a circulating water bath inside individual heating jackets which are connected to a thermostat heating bath to preserve constant temperature throughout the experiment.

Detailed Procedure

The following procedure is the detailed procedure conducted in the Unit Operation Lab of Chemical Engineering Department located at 03-00-06. They are repeated for each run except for A (Start Up) and G (Shut Down) which are carried out to start and end every session.

A. Start Up

i. The main power sources on the computer, temperature and pressure indicator, metering pump and water bath are switched on.
ii. The gas cylinders of N_2 and CO_2/CH_4 are opened.
iii. Set the desired temperature from the thermostat heating bath and open the valves to allow water circulation to begin. Once the desired temperature is reached it will be maintained throughout the experiment.

B. Purging EC with H_20 and N_2

i. Open the inlet valve to the EC as well as the outlet valve. Add H_2O to the syringe and pump it to the EC to allow any remaining substance to be washed out. Close respective valves upon completion.
ii. Open V_{22} and V_{19} to allow N_2 to flow to EC. Open outlet valve from EC to allow the purging to occur. Do this for 1 minute. Close respective valves.

C. Vacuum EC

i. Open V_{19} and V_{24}, then switch on vacuum pump. Once pressure reaches 0.6 bar turn the pump off and close the valves.

D. Gas injection (CO_2 or CH_4)

i. Open $V_1(CO_2)$ or $V_6(CH_4)$ then open V_{14}, V_{13} and then the booster valve. This will then boost the gas to the desired pressure. Once the desired pressure is reached close the respective valves.

E. Injection of Solvent

i. Inject the 5ml solvent into the sample holder and then pump it to the EC by opening the inlet valve.
ii. Turn the pump off and close the respective valve.

F. Transfer gas to EC

i. Ensuring that P1 reading has been taken, transfer gas from the mixing vessel to the EC by opening V15.
ii. Once the pressure in the EC and the mixing vessel is the same, close the vessel.
iii. Wait for the pressure to reach equilibrium and take down P2.

G. Shut Down

i. EC is washed with distillate water and purged with N_2.
ii. At the computer, 'Exit' and Yes' is clicked to exit the software.
iii. Computer is shut off.
iv. The power sources on the computer, temperature and pressure indicator metering pump and water bath are switched off.
v. Close all the gas cylinders and check that all valves are closed.

3.2.3 Data Analysis and Calculation

The amount of CO_2 gas can be determined by applying the Ideal Gas Law equation (Equation 3.1). It relates pressure, temperature and volume of the ideal or perfect gas which can be a good approximation to the behaviour of the gas.

$$PV = nRT \tag{3.1}$$

Where, P = Absolute pressure = Gauge pressure + Atmospheric pressure

V = Volume of gas

n = Number of moles of CO_2 gas

R = Universal gas constant = 0.08314 bar.L/mol.K

T = Absolute temperature

However, the Ideal Gas Law is only accurate at relatively low pressures and high temperatures. It also does not apply to all gases under all conditions (www.everyscience.com, 2004). Hence, in order to consider for the deviation from the ideal condition, another factor is included. It is called the Gas Compressibility Factor, Z, which can be obtained from Aspen HYSYS or the compressibility factor chart. This correction factor is dependent on the pressure and temperature for each gas being considered, as some gases are not ideal even at atmospheric pressure and ambient temperature. If Z is equal to unity, the gas is perfectly ideal whereas for real gases, Z can be either lower or higher than 1. Thus, Equation 3.1 becomes the True Gas Law or the Non-Ideal Gas Law, which is as follows:

$$PV = ZnRT \tag{3.2}$$

The calculation method and equation to be used in this experiment are based on research done by (Vahidi et al, 2009). The calculation is based around four equations that calculate the moles of CO_2 in the gas phase, the moles of CO_2 remaining in the gas phase, the moles of CO_2 in the solvent and the CO_2 loading in the solvent.

The first equation (Equation. 3.3) is to calculate the moles of CO_2 at the starting of the experiment. Using the pressure difference of the initial pressure of the

mixing vessel (MV), denoted as P_1 to the initial pressure of the EC, denoted as P_2, the moles of CO_2 introduced to the system can then be calculated.

$$n_{CO_2} = \frac{V_T}{RT_a}\left(\frac{P_1}{Z_1} - \frac{P_2}{Z_2}\right) \quad (3.3)$$

V_T denotes the volume of the gas container. Z_1 and Z_2 are the compressibility factor corresponding to the initial pressure P_1 and the final Pressure P_2. T_a is the ambient temperature.The number of moles in the gas phase in the EC can be calculated using the equilibrium pressure, P_{eqm}. The second equation (Equation. 3.4) is to calculate the moles of CO_2 remaining in the gas phase.

$$n^g{}_{CO_2} = \frac{(V_{EC} - V_{solvent})P_{eqm}}{ZRT} \quad (3.4)$$

The third equation (Equation. 3.5) will be used to calculate the moles of CO_2 left in the decane.

$$n^*{}_{CO_2} = n_{CO_2} - n^g{}_{CO_2} \quad (3.5)$$

The last equation (Equation. 3.6) is to calculate the CO_2 loading in the decane

$$a_{CO_2} = \frac{n^*CO_2}{n_{solvent}} \quad (3.6)$$

$$n_{solvent} = \frac{mass\ of\ decane}{MW\ of\ decane} \quad (3.7)$$

From the number of moles of CO_2 absorbed, the concentration of the absorbed CO_2 gas by the solvent, C_{CO2} can be calculated using equation 3.8 below:

$$C_{CO_2} = \frac{n^*CO_2}{V_{solvent}} \quad (3.8)$$

Equation 3.9 will be used to calculate Henry's constant of CO_2 in decane based on Henry's Law. P is the pressure and C is the concentration of the gas.

$$k_H = \frac{P_{eqm}}{C_{CO_2}} \quad (3.9)$$

The same equations will be used to calculate the CH_4 loading in the decane and Henry's constant of CH_4 in decane.

FIGURE 3.8 below summarizes the whole methodology for the research investigation.

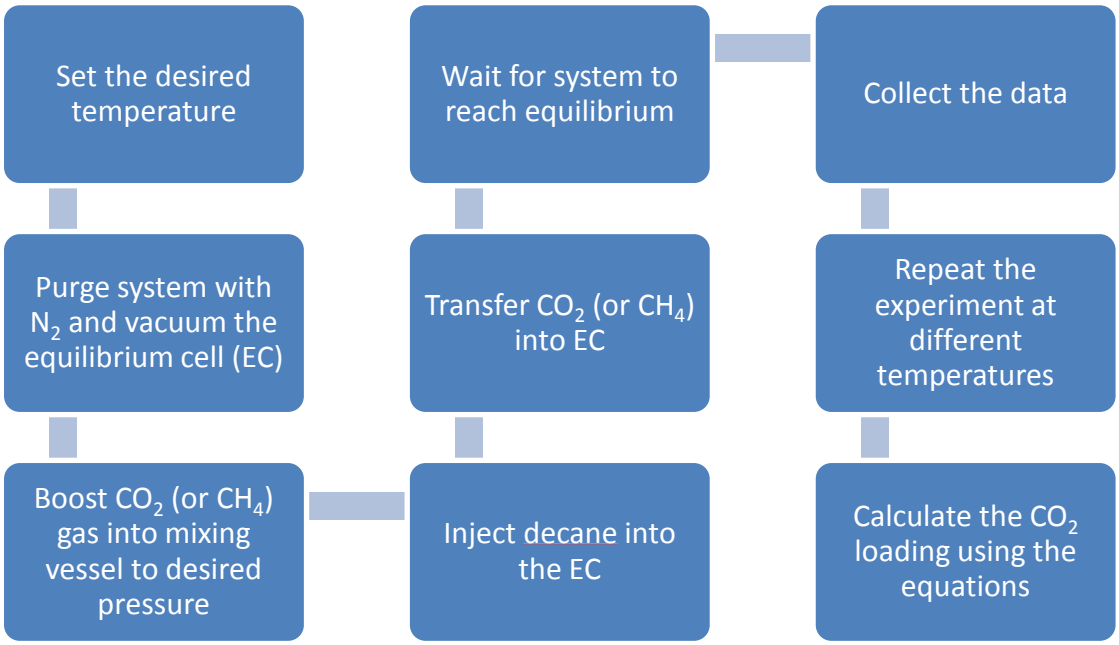

FIGURE 3.8: Summary of Methodology

3.3. Key milestones and Gantt chart

3.3.1 Key Milestones

Several key milestones for this research project must be achieved in order to meet the objective of this project:

FIGURE 3.9: Research Flow Chart

3.3.2 Gantt Chart

TABLE 3.1 and **TABLE 3.2** below outline the Gantt chart for FYP 1 and FYP 2 respectively. The Gantt chart also displays the key milestones for this particular research project.

TABLE 3.1: Gantt Chart FYP I

No.	Detail/Week	1	2	3	4	5	6	7	8	9	10	11	12	13	14
1	Preliminary research work														
2	**Extended Proposal Submission**														
3	**Proposal Defense**														
4	**Introduction to HYSYS simulation software**														
5	**HYSYS Preliminary Process Simulation**														
6	**PR-EOS Simulation**														
7	**SRK -EOS Simulation**														
8	**Interim Report Submission**														

TABLE 3.2: Gantt Chart for FYP II

No.	Detail/Week	15	16	17	18	19	20	21	22	23	24	25	26	27	28
1	**Experiment Progress**														
2	**Experiment setup & initiation**														
3	**CO_2 solubility in decane - 30 bar**														
4	**CH_4 solubility in decane - 30 bar**														
5	**Evaluation of Project Progress**														
6	**Submission of FYP Progress Report**														
7	**Data Analysis and interpretation**														
8	**CO_2 solubility in decane - 10 bar**														
	Report Writing and evaluation														
9	**Oral Presentation**														
10	**Submission of Project Dissertation (Hard Bound) and technical paper**														

CHAPTER 4

RESULTS AND DISCUSSION

4.1. Results

This section of the report gives a clear overview and analysis of the results that were obtained from the project as well as shows the calculations based on the solubility experiment. Gathering of the results was from the solubility experiment conducted using the SOLTEQ High Pressure Gas solubility cell. For this investigation only the 30 bar experiments have been conducted at the various temperatures for both the CO_2 and the CH_4, and additional experiments were done for CO_2 at 10 bar.

4.1.1 Experimental Data

TABLE 4.1 on the following page shows the data obtained from the solubility experiments that were done using the SOLTEQ High Pressure Gas Solubility Cell. The CO_2 experiments were conducted at 10 and 30 bar, and for CH_4 the experiments were conducted at 30 bar. The temperatures investigated were 308.15, 318.15 and 328.15 K. This data will be used to calculate the CO_2 loading in the decane.

TABLE 4.1: Data from the solubility experiment

T(K)	P_1 (bar)	P_2(bar)	P_{eqm} (bar)
		CO_2 (10 bar)	
308.15	10.00	9.72	8.43
318.15	9.98	9.74	8.84
328.15	10.01	9.76	9.12
		CO_2 (30 bar)	
308.15	29.99	29.56	26.52
318.15	30.00	29.59	27.00
328.15	30.03	29.61	28.28
		CH_4 (30 bar)	
308.15	30.00	29.38	27.63
318.15	30.00	29.39	27.90
328.15	30.00	29.36	28.56

4.1.2 CO_2 Loading calculation

Taking the data for 308.15K = 35^{o}C. The moles of CO_2 at the start of the experiment (using equation 3.3) are calculated below.

Data:

T = 308.15 K R = 0.08314 Lbar/Kmol

Z_1 = 0.8394 Z_2 = 0.8416

V_T = 3L

$$n_{CO_2} = \frac{3L}{(0.08314 Lbar/K.mol)(308.15K)}\left(\frac{29.99}{0.8394} - \frac{29.56}{0.8416}\right)$$

Based on the calculation above the number moles of CO_2 initially are 0.0707

Now, calculating the number of moles of CO_2 remaining in the gas phase using Equation 3.4 is as follows.

Data:

T = 308.15 K R = 0.08314 Lbar/Kmol

Z = 0.8593

Vg = $V_{EC} - V_{solvent}$ = (0.05-0.005) L = 0.045L

$$n^{g}{}_{CO_2} = \frac{0.045L.\,26.57bar}{(0.8593)(0.08314Lbar/K.mol)(308.15K)}$$

From the calculation the number of moles of CO_2 remaining in the gas phase is 0.0543

The number of moles left in the decane is then calculated using equation 3.5.

$n^{*}{}_{CO_2} = 0.0707 - 0.0543$ = 0.0164 moles

CO_2 loading in the decane (using Equation 3.7) is then calculated to be:

$$a_{CO_2} = \frac{0.0164}{0.02565}$$

The CO_2 loading in the decane at 308.15K and 30 bar is 0.6393

The same procedure is followed to calculate the CH_4 loading in the decane solvent.

TABLE 4.2: CO_2 loading in decane from the experimental data

	T(K)	P_1 (bar)	CO_2 Loading
	308.15	10.00	0.2231
10 bar	**318.15**	9.98	0.1974
	328.15	10.01	0.1761
	308.15	29.99	0.6393
30 bar	**318.15**	30.00	0.5621
	328.15	30.03	0.4982

TABLE 4.3: CH_4 loading in decane from the experimental data

T(K)	P_1 (bar)	CH_4 Loading
308.15	30.00	0.2128
318.15	30.00	0.1943
328.15	30.00	0.1769

4.1.3 HYSYS Simulation results

TABLE 4.4 and **TABLE 4.5** below show the comparison between the HYSYS simulation results and the solubility experiment results for the CO_2 loading calculation. The comparison is done for the experiments for 10 and 30 bar, at temperatures of (308.15, 318.15 and 328.15) K, respectively.

TABLE 4.4: Comparison of experiment result and simulation result (10 bar)

T(K)	CO_2 Loading		
	Experiment Result	**Simulation Result (PR-EOS)**	**Simulation Result (SRK-EOS)**
308.15	0.2231	0.1315	0.1275
318.15	0.1974	0.116071	0.1132
328.15	0.1761	0.103864	0.1018

TABLE 4.5: Comparison of experiment result and simulation result (30 bar)

T(K)	CO_2 Loading		
	Experiment Result	**Simulation Result (PR-EOS)**	**Simulation Result (SRK-EOS)**
308.15	0.6393	0.4863	0.4689
318.15	0.5621	0.4134	0.4017
328.15	0.4982	0.3604	0.3524

APPENDIX A and **APPENDIX B** show the extended CO_2 loading and CH_4 loading results from the HYSYS simulation data. The results are for (308.15, 318.15 and 328.15) K at pressures ranging from 10 bar until 60 bar. **APPENDIX C** shows the Henry's constant data for the simulation results for both CO_2 and CH_4 and **APPENDIX D** shows all the simulation data for this system.

4.2 Discussion

In this investigation, the physical solubility of CO_2 in n-decane is investigated from a binary system with CH_4 at different compositions and are determined at varying temperatures, namely (308.15, 318.15 and 328.15) K and pressures (10, 30 and 45) bar**.**

For the experimental results, upon observation of the results several points can be further discussed to see if it will be possible to meet the objectives set for this research investigation. Due to time constraints the experiments were only conducted for 8 hours versus the required 24 hours that are generally required for solubility experiments conducted at high pressure. For this semester there were four students using the equipment for the experiment, which meant limited time for experimentation. In that regard, it was decided to only focus on one pressure and investigate its changes at the various temperatures for both CO_2 and CH_4 respectively. Then further experiments were conducted for CO_2 at a lower pressure of 10 bar for the pressure relationship.

Based on the literature investigation it was established that the most favourable HYSYS fluid packages to use for this process simulation were the Peng Robinson equation of state (PR-EOS) and the Soang-Redlich Kwong equation of state (SRK-EOS) as they present the most accurate results as compared to experiments that have been conducted involving organic compounds and their behaviour (Karim et al., 2010). As there was insufficient time for experimentation it will be necessary to lean more on the simulation results of the investigation, more than the experimental results. That being said, there was still enough data from the solubility experiment to make some conclusions and comparisons with the simulation data.

4.2.1 CO_2 and CH_4 Loading based on solubility experiment

FIGURE 4.1 below depicts the CO_2 loading in decane from the results that were obtained from the equilibrium pressure solubility experiments. The pressures used were 10 and 30 bar and the temperature was varied. From **FIGURE 4.1** it can be noted that the CO_2 loading was higher than CH_4 loading. The CO_2 loading was 64.5 – 66.7% higher than the CH_4 loading, decreasing with a rise in temperature.

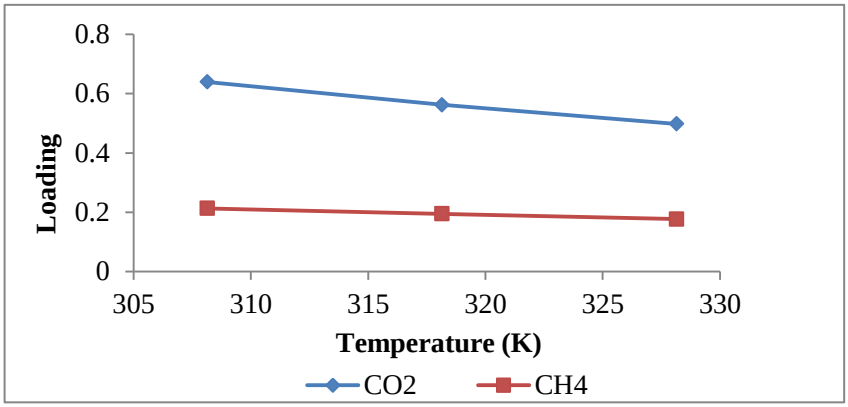

FIGURE 4.1: CO_2/CH_4 loading in decane from the solubility experiment

FIGURE 4.2 below, the CO_2 loading at 10 and 30 bar is shown. The graph clearly shows that the CO_2 loading was higher for the 30 bar experiments than the 10 bar experiments. It was found that at 308.15K the CO_2 loading was 65.1% higher at 30 bar than 10 bar, at 318.15K it was 64.9% higher and at 328.15K it was 64.6% higher. The CO_2 loading was 22.4% and 22.1% higher at 308.15K than at 328.15K for a pressure of 10 and 30 bar, respectively. The trend from the experiment is consistent with a higher loading for a lower temperature and a higher pressure (Reger et al., 2009)

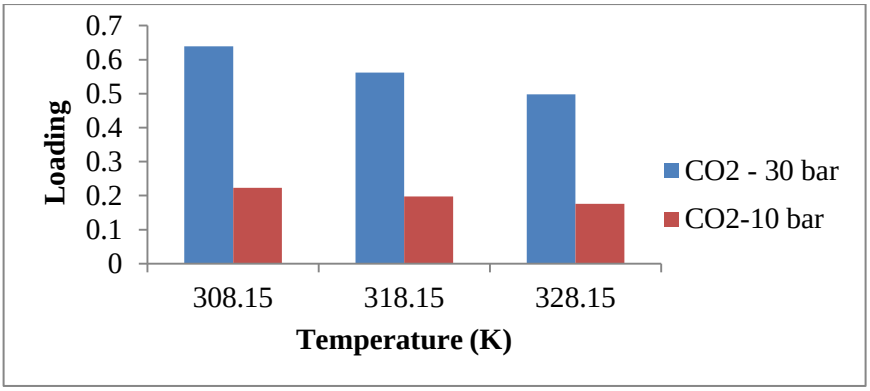

FIGURE 4.2: Pressure relationship with CO_2 loading from the solubility experiment

4.2.2 Comparison between Experiment result and Simulation result

FIGURE 4.3 shows the difference between the CO_2 loading gained from the experimental results and the CO_2 loading calculated by the HYSYS simulation at 10 and 30 bar. For the simulation, the CO_2 loading results for PR-EOS were between 2.2-3.5% higher than the SRK-EOS, thus giving a better result. The range goes from the highest temperature to the lowest temperature respectively.

FIGURE 4.3 also shows the difference between the CO_2 loading gained from the experimental results and the CO_2 loading calculated by the HYSYS simulation at 10 and 30 bar. The simulation results for PR-EOS ranged from 0.3604 to 0.4863 for 30 bar, and for the SRK-EOS it ranged from 0.3524 to 0.4689. The range goes from the highest temperature to the lowest temperature respectively. As for the experimental results, the data ranged from 0.4962 to 0.6393 for 30 bar.

It can be observed that the experiment and simulation results have some deviation, however, the results for both are consistent with the expected relationship of temperature to solubility outlined in the literature review which predicted that at lower temperatures and higher pressure the CO_2 loading would be higher (Reger et al., 2009).

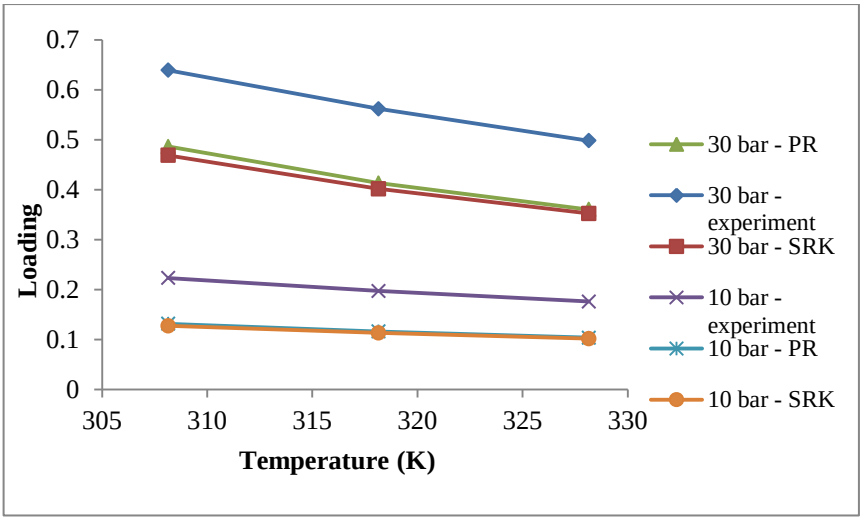

FIGURE 4.3: Comparison between experimental CO_2 loading and simulation

4.2.3 CO_2 Loading in decane using the simulation method

FIGURE 4.4 to **FIGURE 4.6** show the solubility of pure CO_2 in decane solvent at the selected pressures, ranging from 10 bar to 60 bar respectively. The graph y-axis is the CO_2 loading in the solvent at equilibrium and the x-axis are the various temperatures where the experiment is held which as mentioned are (308.15, 318.15 and 328.15) K. The graph shows both the PR-EOS and the SRK-EOS results. The PR-EOS shows a higher solubility of CO_2 in the n-decane solvent. For the purpose of this investigation the PR-EOS is used for comparison as it gives better results.

From the figure it can be seen that the highest CO_2 loading is at 60 bar and that the lowest is at 10 bar. This is the trend for all the temperatures that were investigated. **FIGURE 4.7** puts all the respective graphs on one axis for a comparison. The graph shows that there is more absorption at lower temperatures (308.15K) and the highest pressure (60 bar). The reason for this is that under conditions of lower temperatures and higher pressures the gas molecules will have more collisions and enter the liquid solvent more readily (Ebbing & Gammon, 2010).

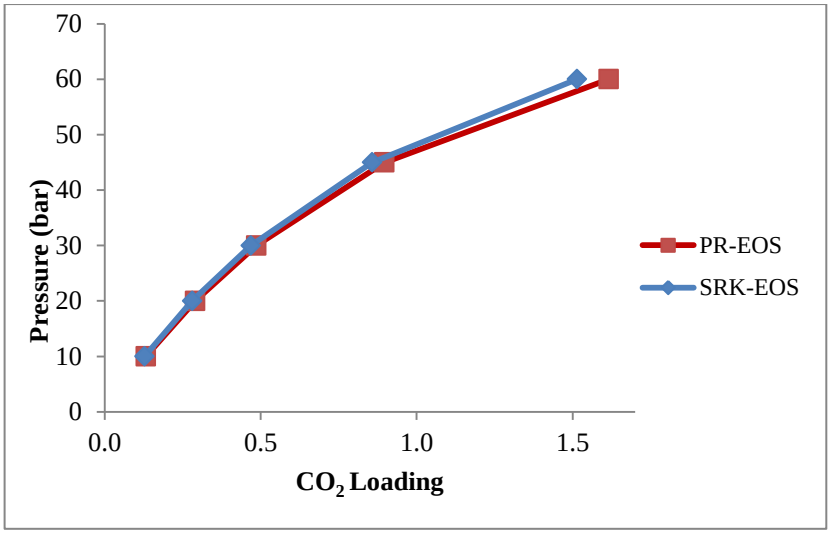

FIGURE 4.4: CO_2 loading at 308.15K

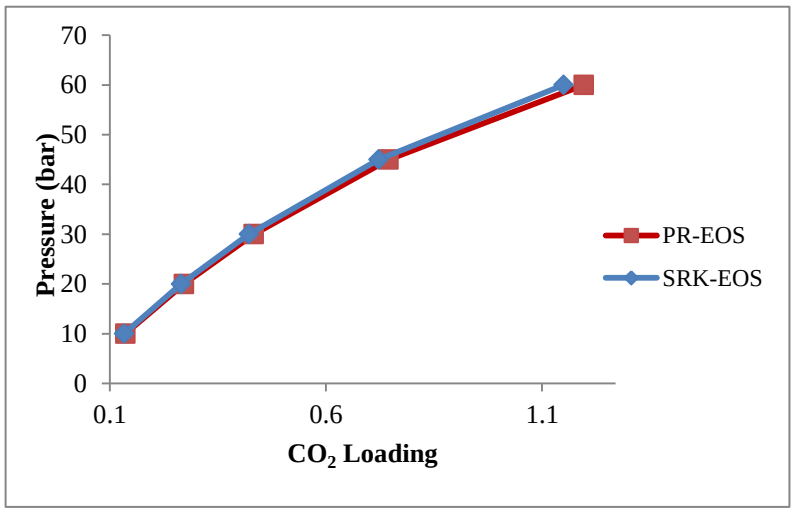

FIGURE 4.5: CO_2 loading at 318.15K

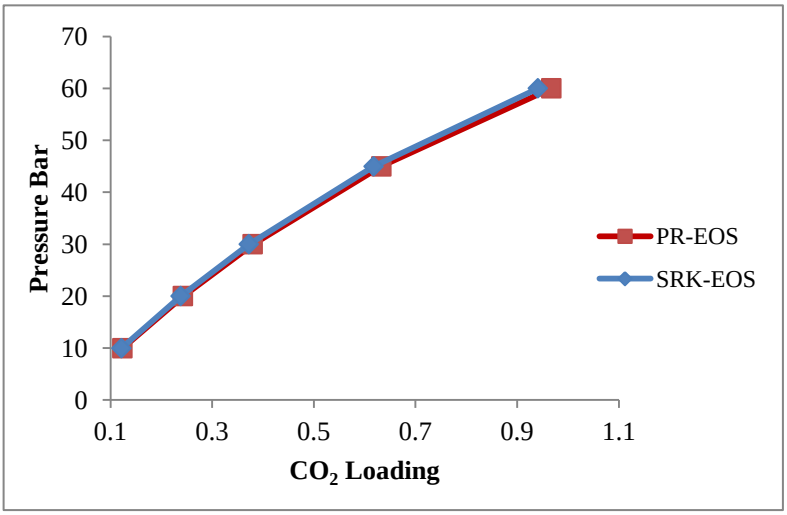

FIGURE 4.6: CO_2 loading at 328.15K

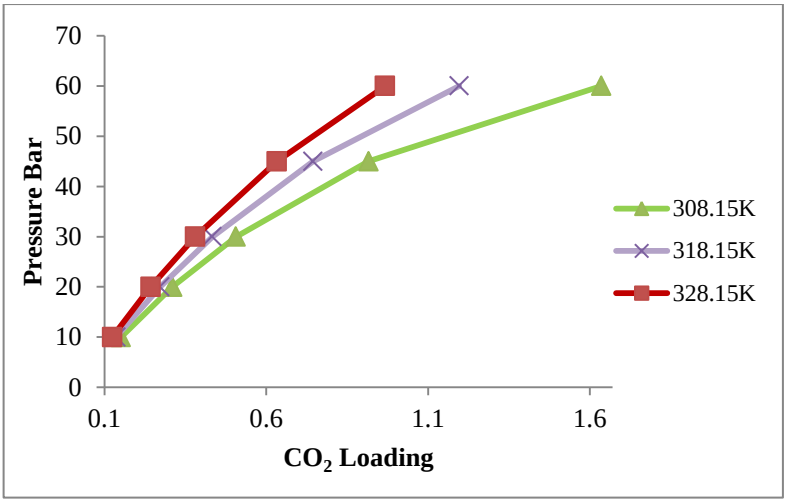

FIGURE 4.7: CO_2 Loading at different temperatures

4.2.4 CH_4 Loading in decane using the simulation method

FIGURE 4.7 to **FIGURE 4.9** shows the solubility of pure CH_4 in the decane solvent at the selected pressures, ranging from 10 bar to 60 bar respectively. The graph y-axis is the CO_2 loading in the solvent at equilibrium and the x-axis are the various temperatures where the experiment is held which as mentioned are (308.15, 318.15 and 328.15) K. The graph shows both the PR-EOS and the SRK-EOS results.

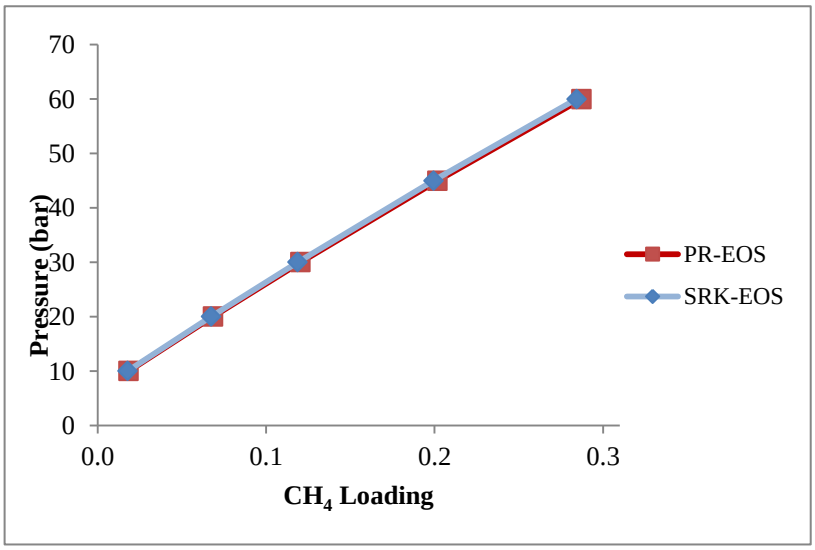

FIGURE 4.8: CH_4 loading at 308.15K

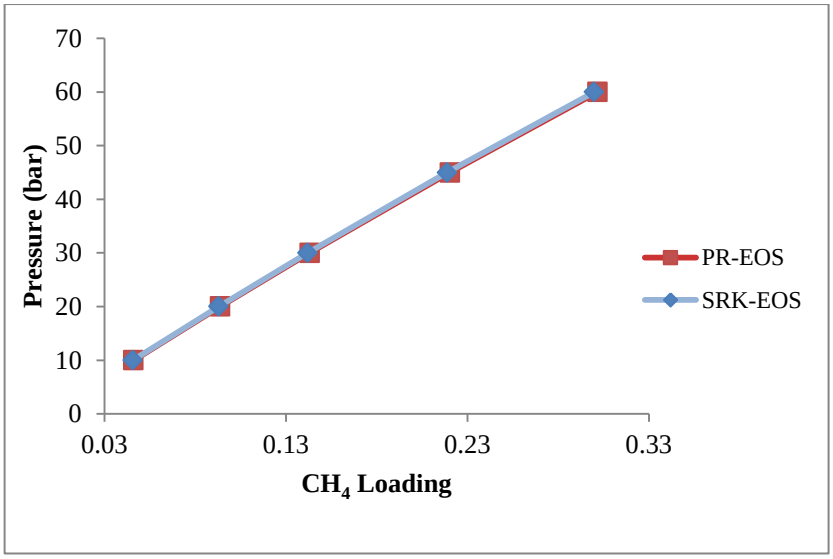

FIGURE 4.9: CH_4 loading at 318.15K

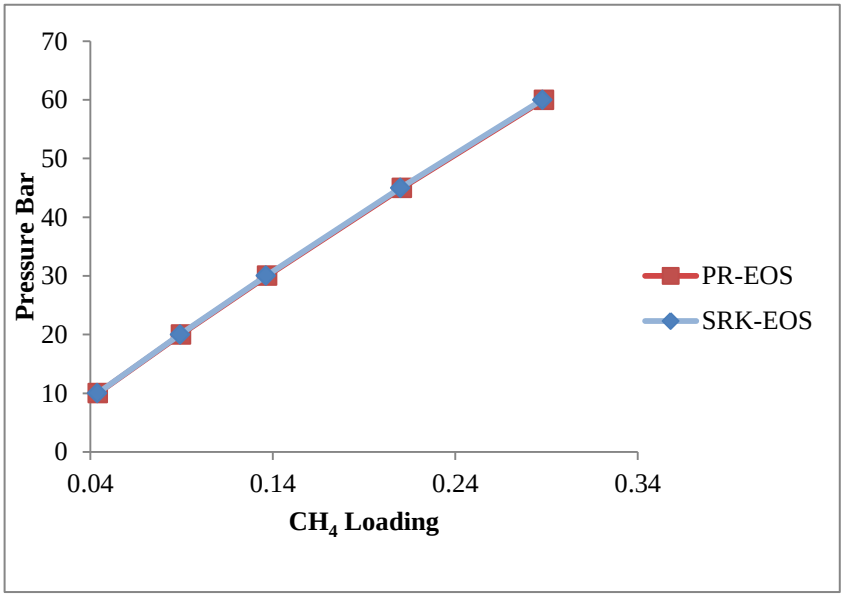

FIGURE 4.10: CH_4 loading at 328.15K

The trend for the CH_4 is similar to that of the CO_2 trend, in that with increasing pressure there is an increase in the CH_4 loading in the solvent.

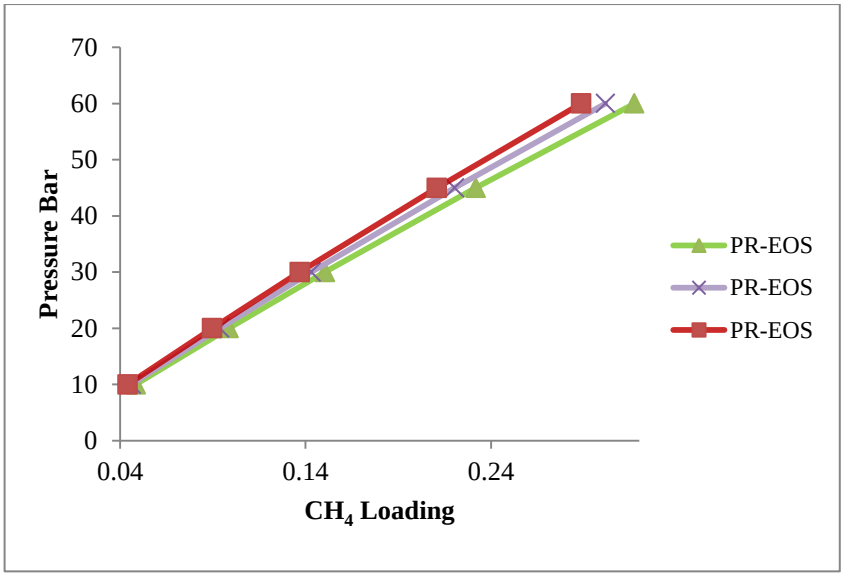

FIGURE 4.11: CH_4 Loading at different temperatures

From the above analysis it can be seen that for both CO_2 and CH_4 an increase from 10 bar to 60 bar resulted in an increase in the solubility of both and the increase of temperature from 308.15K to 328.15K saw a decrease in solubility. Thus, for this system the best results were obtained at 308.15K and 60 bar for both components.

4.2.5 Effect of Temperature and Pressure

As can be seen from **FIGURE 4.11** – at the selected equilibrium pressures, ranging from 10 to 60 bar, it can be noted that as the temperature rises the solubility decreases. This can be explained from the molecular behaviour of the gases from the kinetic molecular theory of gases (Reger et al., 2009). As the temperature rises the kinetic energy of the molecules decreases, which results in less collisions and thus slowing down the absorption of the molecules into the solvent.

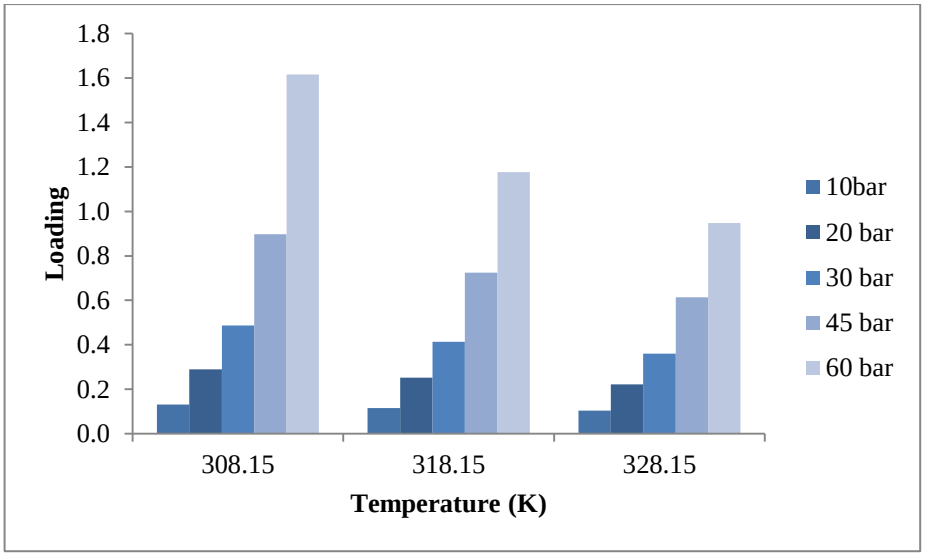

FIGURE 4.12: Effect of temperature on CO_2 Loading

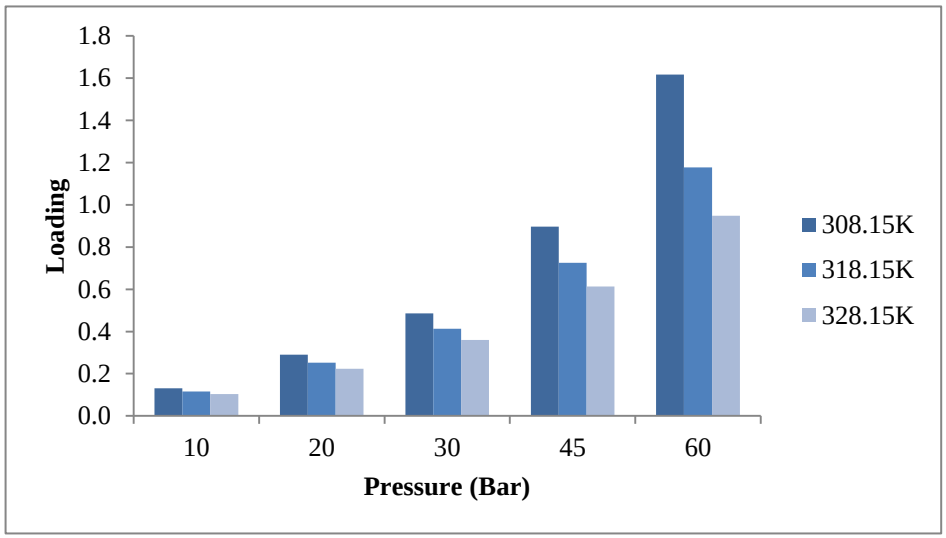

FIGURE 4.13: Effect of pressure on CO_2 Loading

For the pressure relationship, it can be seen that with an increase in pressure there is also a rise in the solubility of the components. It can be observed from the Fig. 9 that the pressure has positive effect on the CO_2 loading. It can be explained on the basis that the liquid pressure inside the cell is directly proportional to the pressure of the gas above the liquid (Ebbing & Gammon, 2010). This can be further explained by the principle of solubility which shows that as pressure increases in a container, more gas molecules will be forced to enter the solvent as there will be less volume for the gas molecules to occupy (Trefil, 2003).

4.2.6 CO_2 and CH_4 loading trend

The solubility of the binary gas system of CO_2 and CH_4 is discussed for various gas molar compositions. Since the values for PR-EOS gave better results than the SRK-EOS, only the PR-EOS results are presented for this analysis.

From the results, it can be noted that, as the concentration of the CO_2 in the feed gas increases, absorption increases, the same can be observed for CH_4 but to a lesser degree. Under binary conditions, where x_{CH4} = 0.5 and x_{CO2}= 0.5, the CH_4 loading was 0.2192 and the CO_2 loading was 0.4253– the CO_2 loading in the decane is 48.4% higher than that of CH_4. At a binary molar feed composition of x_{CO2} = 0.75 and x_{CH4}= 0.25, the CO_2 loading was 0.7803 at 60 bar, on the other hand for x_{CH4} = 0.75, the CH_4 loading was only 0.2733. The CO_2 loading is observed to be 65% higher. Furthermore, for the pure component of CH_4 the maximum loading observed was 0.3173 at 60 bar and 308.15K. For pure CO_2, the highest loading was 1.6157 at the same conditions which is approximately five times the loading of the pure CH_4 at the same parameters.

From this data, it can be observed that decane preferentially absorbs CO_2 as compared to CH_4, which is in agreement with the study done by Ryan-Holmes (GPSA, 2004). **FIGURE 4.13** illustrates the trend of CO_2 and CH_4 loading at various compositions.

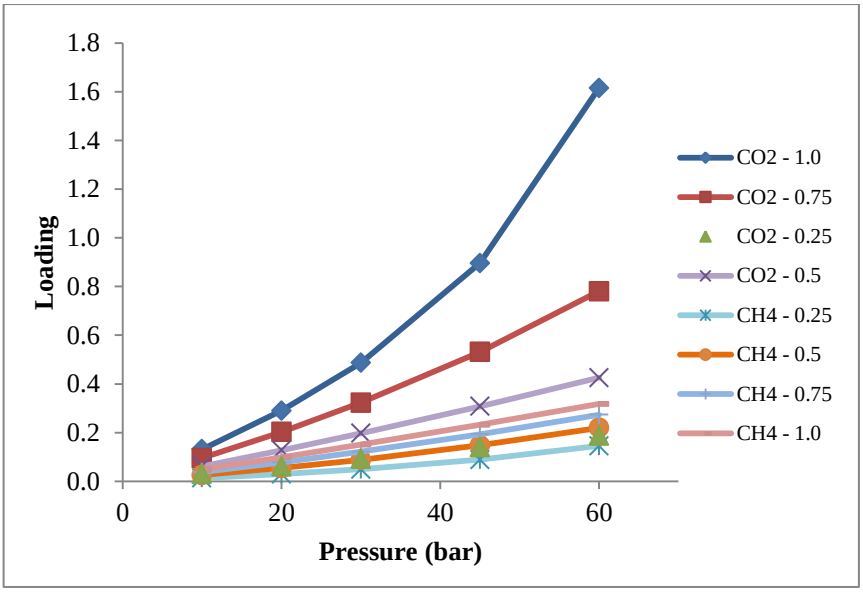

FIGURE 4.13: CO_2 and CH_4 Loading at various compositions.

This can lead to the conclusion that in a binary system, competitive absorption will occur; and that more CO_2 will be absorbed by the decane solvent which is in good agreement with the Ryan-Holmes study on butane, which led to the conclusion that n-alkanes preferentially absorb CO_2 (GPSA, 2004).

4.2.7 Henry's constant and CO_2 and CH_4 loading

The next important factor that needs to be considered is Henry's constant. For gases that do not react with the solvent – as is the case with physical absorption, Henry's law gives the relationship between gas pressure and gas solubility. From **FIGURE 4.14** below depicts the Henry's constant relationship with CO_2 loading in the decane solvent. From the graph it can be seen that the highest Henry's constant is at 328.15K and it decreases as the solubility of CO_2 increases – the same goes for CH_4 in **FIGURE 4.15**. Henry's constant also increases with rise in temperature, in other words solubility decreases with rise in temperature. At constant temperature the amount of gas dissolved in the solvent is directly proportional to the pressure of the gas – as pressure increases so will solubility, in the case of pressure there is an inverse relationship with Henry's constant (Ebbing & Gammon, 2010).

Furthermore, increasing concentration will lead to a decrease in Henry's constant. It can also be seen upon comparison of the two graphs that CH_4 has a much higher Henry's constant than CO_2, this again illustrates that CO_2 has a higher solubility than CH_4 since it is noted that Henry's constant decreases with increasing solubility.

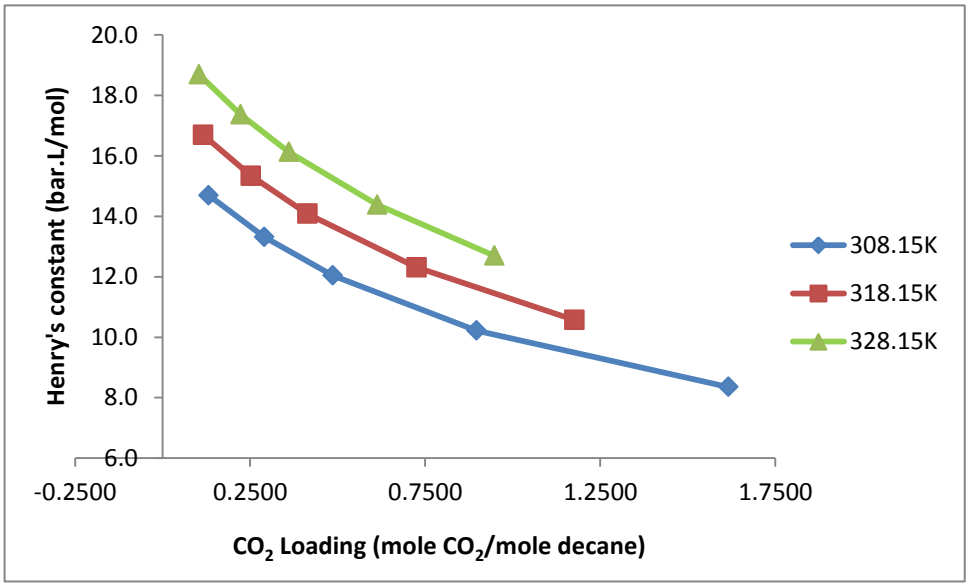

FIGURE 4.14: Henry's constant versus CO_2 Loading

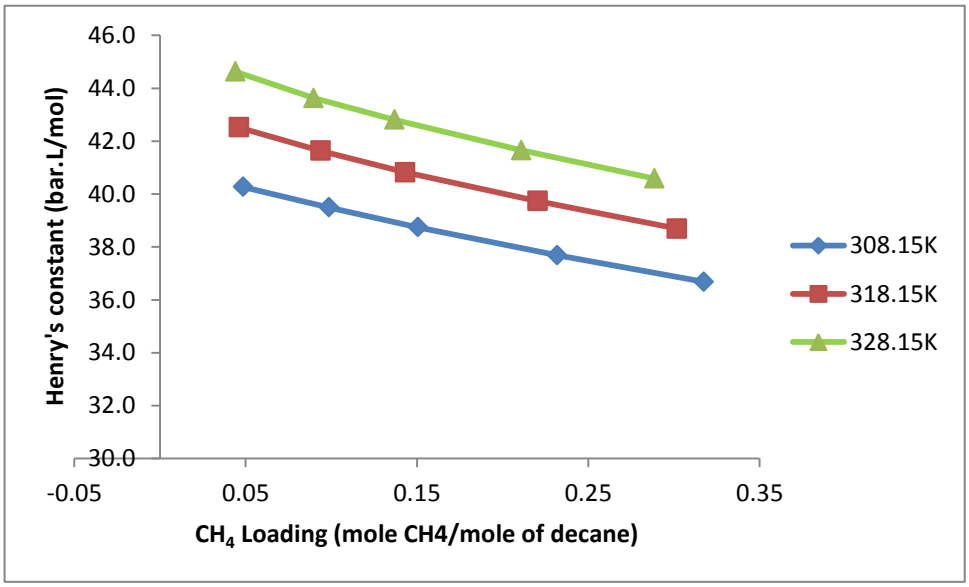

FIGURE 4.14: Henry's constant versus CH_4 Loading

From these discussions, the points that can be summarized are that this process is based on physical absorption theory which from the literature review clearly states that physical solubility favours higher partial pressures and higher concentrations of the gas (Keskes et al, 2006). In this investigation various compositions of CO_2 and CH_4 were investigated at various temperatures and pressures. The results have illustrated that this route of carbon dioxide capture may be a viable one, especially since it is expected that the CO_2 will be at high partial pressures and high concentrations which are the conditions for offshore natural gas fields (Pereira et al., 2011). The relationship for pressure and temperature was found to be in agreement with Henry's Law, which predicts higher solubility for higher partial pressure (Ebbing & Gammon, 2010). The solvent under study, n-decane, has shown favourability towards absorption of the CO_2 vs the CH_4 and this makes it a viable candidate for physical absorption of CO_2 from natural gas streams.

CHAPTER 5

CONCLUSION AND RECOMMENDATIONS

5.1. Conclusion

To conclude the investigation, it can be said that the HYSYS process simulator is a powerful software that chemical engineers can use to predict the behaviour of various chemical and thermodynamic systems. For this investigation the main focus was investigating the physical solubility of a CO_2/CH_4 binary gas system in a decane solvent. CO_2 has been established as a major contributor to greenhouse gas emissions which leads to the phenomenon of global warming.

From the HYSYS results and the solubility experiment the behaviour of the binary gas of CO_2 and CH_4 in the n-decane physical solvent was investigated based on the various parameters imposed for the investigation. The following conclusions were drawn from the experiment:

- The results showed that increasing the pressure and increasing the concentration of CO_2 in the binary feed gas favoured an increase in physical solubility of CO_2.
- The results also showed that there was a decrease in solubility with a rise in temperature.
- Henry's constant showed that a rise in solubility resulted in a decrease in Henry's constant, which is predicted by Henry's law for pressure and temperature relationships with solubility.

However, there is a deviation in the CO_2 and CH_4 loading for the pure components of CO_2 and CH_4 when compared with the simulation results. The Park et al method of calculation assumes an ideal relationship of pressure, volume and temperature. This results in slightly deviated results than the simulation as the HYSYS simulator calculates the properties of the streams using thermodynamic properties depending on the fluid package chosen.

From the data gathered from this investigation the objective has been achieved and the solubility data of this system has been established. The results show that CO_2 has a higher affinity for dissolving in the decane solvent than CH_4. Furthermore increasing the molar composition of the binary feed gas towards a higher CO_2 fraction also favours a higher solubility. Lastly, the solubility shows an increase at lower temperatures and higher pressure for both the CO_2 and the CH_4, but less so for the latter.

5.2 Recommendations

There are several recommendations that can be made with regards to this project in order to achieve better results for this study. The recommendations that have been identified are as follows:

a. Checking Equipment and testing before each experiment

For the SOLTEQ High Pressure Solubility Cell there were a number of individuals that were using the equipment daily. Thus, a frequent check of certain parameters – such as leakage will produce better data for the research.

b. Reproducibility of Results

As it can be seen from the report the results only had one reading – for the sake of validity it will be worth doing the same experiment more than once in order to check for reproducibility of results.

c. Cleaning of Equipment

There should be regular maintanance of the internals of the unit. From discussion with the other students using the equipment it was noted that there are several solvents being used in the equilibrium cell daily and since it is a closed vessel there is no way of gauging what the condition is inside. The wash and purge before and after experiment may not be enough to clean the EC completely and this could lead to erronous results.

d. Adjusting the parameters of the fluid packages

According to Karim et al. (2010) for higher alkanes the reliability of PR-EOS and SRK-EOS decreases, in order for them to give better results the binary interacton parameter must be introduced and adjusted within the system before simulation. This should give more correct results.

REFERENCES

Solubility & Solution in Aqueous Media. (1999). New York: Oxford University Press.

HYSYS 7.2 User's Guide. (2011). Aspen.

Ahmed, T., & Semmens, M. J. (1992). Use of transverse flow hollow fibers for bubble-less membrane . *Membrane Science*, 69.

Arronwilas, A., & Vaewab, A. (2007). Integration of CO2 Capture unit using single and blended amines into supercritical coal-fired power plants: implications for emission and energy management. *International Journal Greenhouse Gas Control*, 143-150.

Association, G. P. (2004). *GPSA Engineering Data Book, 12th Edition.* GPSA Press.

Battino, R., & Clever, H. L. (1966). The Solubility of Gases in Liquids. *Chemical Reviews*, 395-463.

BBC News. (n.d.). Retrieved February 8, 2013, from BBC News: http://news.bbc.co.uk

Browning, G. J., & Weiland, R. H. (1994). Physical Solubility of Carbon Dioxide in Aqueous Alkanolamines via Nitrous Oxide Analogy. *Journal of Chemical & Engineering Data*, 817-822.

Burr, B., & Lyddon, L. (2008). *A Comparison of physical solvents for Acid Gas Removal.* Texas: Gas Processors' Association Convention.

Burr, B., & Lyddon, L. (n.d.). *A comparison of physical solvents for acid gas removal.* Bryan, Texas: Bryan Research & Engineering, Inc.

Chung, P.-Y., Soriano, A. N., Leron, R. B., & Li, M.-H. (2010). Equilibrium solubility of carbon dioxide in the amine solvent system of (triethanolamine + piperazine + water). *Sciencedirect*, 802-807.

Desideri, U., & Paolucci, A. (1999). Performance modeling of a carbon dioxide removal system for power plants. *Energy Conversion Management*, 40.

Dubey, M. K., Ziock, H., Rueff, G., Elliot, S., Smith, W. S., Lackner, K. S., & Johnston, N. A. (2002). Extraction of carbon dioxide from the atmosphere through engineered chemical sinkage. *Abstracts of papers of the American Chemical Society*, 577-578.

Dunyushkin, I. I., Skripka, V. G., & Nenartovich, T. L. (1977). Phase Equilibria in the carbon dioxide/n-butane/n-decane and carbon dioxide/methane/n-decane. *VINITI*, 1-5.

Ebbing, D. D., & Gammon, S. D. (2010). *General Chemistry, Enhanced Edition.* Cengage Learning.

Georgiadis, M. C., & Pistikopoulos, E. N. (2008). *Energy Systems Engineering*. Weinheim: Wiley-Vch Verlag GmbH & Co.

Gupta, M., Coyle, I., & Thambimuthu, K. (2003). CO2 Capture technologies and Opportunities in Canada. *1st Canadian CC&S Technology Roadmap Workshop* (pp. 1-36). Alberta, Canada: CANMET Energy Technology Centre.

Helmenstine, A. M. (n.d.). *About.com*. Retrieved April 6, 2013, from About.com: http://chemistry.about.com/od/solutionsmixtures/a/solubility-rules.htm

Holmes, A. S., & Ryan, J. M. (1979). *Patent No. U.S.4318732.* United States.

Jou, F. Y., Deshmukh, R. D., & Mather, A. E. (1990). Solubility of hydrogen sulfide, carbon dioxide, methane, and ethane in sulfolane. . *Fluid Phase Equilibria*, 313-324.

Karim, A. A., Abdel-Rahman, Z. A., & Hadi, A. J. (2010). Solubility prediction of CO2 in several liquid solvents using CHEMCAD and HYSYS simulators. *Diyala Journal of Engineering Sciences*, 356-373.

Kariznovi, M., Nourizieh, H., & Abedi, J. (2013). Experimental results and thermodynamic investigation of carbon dioxide solubility in heavy liquid hydrocarbons and corresponding phase properties. *Fluid Phase Equilibria (ScienceDirect)*, 105-111.

Keskes, E., Adjiman, C. S., Galindo, A., & Jackson, G. (2006). *A Physical Absorption Process for the Capture of Carbon Dioxide from Carbon Dioxide-Rich natural gas streams.* London, UK: Chemical Engineering Department, Imperial College London.

Kohl, A. L., & Nielsen, R. (2005). *Gas Purification.* New York: Gulf Professional Publishing.

Kohl, A. L., & Nielsen, R. B. (1997). *Gas purification, 5th Edition.* New York: Gulf Publishing Company.

Lepaumier, H., Picq, D., & Carrette, P. L. (2010). CO2 capture: why, how, with what constraints? *Web of Science*, 36-40.

Murrieta-Guevara, F., Romero-Martinez, A., & Terjo, A. (1988). Solubilites of Carbon Dioxide and hydrogen sulfide in propylene carbonate, n-methylpyrrolidone and sulfolane. . *Fluid Phase Equilibria*, 105-115.

Newman, S. (1985). *Acid and sour gas treating processes, 1st Edition.* New York : Gulf Publishing Company.

Nourozieh, H., Kariznovi, M., & Abedi, J. (2013). Measurement and correlation of saturated liquid and gas solubility for decane, tetradecane and their binary mixtures saturated with carbon dioxide. *Fluid Phase Equilibria (ScienceDirect)*, 246-254.

Padurean, A., Cormos, C., Cormos, A., & Agachi, P. (2011). Multicriterial analysis of post-combustion carbon dioxide capture using alkanolamines. *International Journal of Greenhouse Gas Control*, 676-685.

Park, M. K., & Sandall, O. C. (2001). Solubility of Carbon Dioxide and Nitrous Oxide in 50% mass Methyldiethanolamine. *Journal of Chemical Engineering Data, 46*, 166-168.

Pereira, F. E., Keskes, E., Galindo, A., Jackson, G., & Adjiman, C. S. (2011). Integrated solvent and process design using a SAFT-VR thermodynamc description: High Pressure Separation of carbon dioxide and methane. *Computers & Chemical Engineering*, 474-491.

Portugal, A. F., Sousa, J. M., Magalhaes, F. D., & Mendes, A. (2009). Solubility of carbon dioxide in aqueous solutions of amino acid salts. *ScienceDirect*, 1993-2002.

Reger, D. L., Goode, S. R., & Ball, D. W. (2009). *Chemistry: Principles and Practice.* Cengage Learning.

Saylor, J. H., Stuckey, J. M., & Gross, P. M. (1938). The Validity of Henry's Law for the Calculation of Vapour Solubilities. *Chemical Reviews*, 373-376.

Stanford University. (2005). *An Assessment of Carbon Capture Technologies and Research Opportunities.* Global Climate and Energy Project.

Tan, L. S., Murshid, G., Bustam, M. A., Lau, K. K., & Shariff, A. M. (2011). Solubility and absorption perfomance of enhanced amine solvent (stonvent) for carbon dioxide removal. *International Journal of Chemical and Environmental Engineering*, 221-226.

Trefil, J. S. (2003). *The Nature of Science: An A-Z Guide to the Laws and Principles Governing Our Universe.* Boston: : Houghton Mifflin.

University of Florida. (n.d.). Retrieved April 1, 2013, from University of Florida: http://itl.chem.ufl.edu/2041_f97/lectures/lec_i.html

Vahidi, M., Matin, N. S., Goharrokhi, M., Jenab, M. H., Abdi, M. A., & Najibi, S. H. (2009). Correlation of CO2 solubility in N-methyldiethanolamCorrelation of CO2 solubility in N-methyldiethanolamine;piperazine aqueous solutions using extended Debye–Hückel model. *The Journal of Chemical Thermodynamics*, 1272-1278.

Volland , W. (n.d.). Retrieved March 15, 2013, from http://www.800mainstreet.com/9/0009-006-henry.html

White , C. M., Strazisar, B. R., Granite, E. J., & Hoffman, J. S. (2003). Separation and capture of CO2 from large stationary sources and sequestration in geological formations - coalbds and deep saline aquifiers. *Journal of Air and Waste Management Association*, 645-715.

Yalkowsky, S. H. (1999). *Solubility & Solution in Aqeous Media.* New York: Oxford University Press.

APPENDICES

APPENDIX A – CO_2 Loading Results – HYSYS Simulation

TABLE A1: CO_2 Loading in decane at 308.15K (PR-EOS)

P(bar)	$nC_{10}H_{22}$	nCO_2	CO_2 Loading
10	0.8838	0.1162	0.1315
20	0.7752	0.2248	0.2900
30	0.6728	0.3272	0.4863
45	0.5273	0.4727	0.8965
60	0.3823	0.6177	1.6157

TABLE A2: CO_2 Loading in decane at 318.15K (PR-EOS)

P(bar)	$nC_{10}H_{22}$	nCO_2	CO_2 Loading
10	0.8960	0.1040	0.1161
20	0.7988	0.2012	0.2519
30	0.7075	0.2925	0.4134
45	0.5797	0.4203	0.7250
60	0.4595	0.5405	1.1763

TABLE A3: CO_2 Loading in decane at 328.15K (PR-EOS)

P(bar)	$nC_{10}H_{22}$	nCO_2	CO_2 Loading
10	0.9059	0.0941	0.1039
20	0.8178	0.1822	0.2228
30	0.7351	0.2649	0.3604
45	0.6199	0.3801	0.6131
60	0.5135	0.4865	0.9474

TABLE A4: CO_2 Loading in decane at 308.15K (SRK-EOS)

P(bar)	$nC_{10}H_{22}$	nCO_2	CO_2 Loading
10	0.8869	0.1131	0.1275
20	0.7809	0.2191	0.2806
30	0.6808	0.3192	0.4689
45	0.5384	0.4616	0.8574
60	0.3978	0.6022	1.5138

TABLE A5: CO_2 Loading in decane at 318.15K (SRK-EOS)

P(bar)	$nC_{10}H_{22}$	nCO_2	CO_2 Loading
10	0.8983	0.1017	0.1132
20	0.8030	0.1970	0.2453
30	0.7134	0.2866	0.4017
45	0.5877	0.4123	0.7015
60	0.4696	0.5304	1.1295

TABLE A6: CO_2 Loading in decane at 328.15K (SRK-EOS)

P(bar)	$nC_{10}H_{22}$	nCO_2	CO_2 Loading
10	0.9076	0.0924	0.1018
20	0.8209	0.1791	0.2182
30	0.7394	0.2606	0.3524
45	0.6257	0.3743	0.5982
60	0.5205	0.4795	0.9211

APPENDIX B – CH_4 Loading Results – HYSYS Simulation

TABLE B1: CH_4 Loading in decane at 308.15K (PR-EOS)

P(bar)	$nC_{10}H_{22}$	nCH_4	CH_4 Loading
10	0.9538	0.0462	0.0484
20	0.9103	0.0897	0.0985
30	0.8692	0.1308	0.1505
45	0.8118	0.1882	0.2318
60	0.7591	0.2409	0.3173

TABLE B2: CH_4 Loading in decane at 318.15K (PR-EOS)

P(bar)	$nC_{10}H_{22}$	nCH_4	CH_4 Loading
10	0.9560	0.0440	0.0460
20	0.9143	0.0857	0.0937
30	0.8748	0.1252	0.1431
45	0.8194	0.1806	0.2204
60	0.7682	0.2318	0.3017

TABLE B3: CH_4 Loading in decane at 328.15K (PR-EOS)

P(bar)	$nC_{10}H_{22}$	nCH_4	CH_4 Loading
10	0.9578	0.0422	0.0440
20	0.9177	0.0823	0.0897
30	0.8796	0.1204	0.1369
45	0.8259	0.1741	0.2108
60	0.7760	0.2240	0.2887

TABLE B4: CH_4 Loading in decane at 308.15K (SRK-EOS)

P(bar)	$nC_{10}H_{22}$	nCH_4	CH_4 Loading
10	0.9544	0.0456	0.0478
20	0.9113	0.0887	0.0973
30	0.8705	0.1295	0.1488
45	0.8134	0.1866	0.2294
60	0.7608	0.2392	0.3144

TABLE B5: CH_4 Loading in decane at 318.15K (SRK-EOS)

P(bar)	$nC_{10}H_{22}$	nCH_4	CH_4 Loading
10	0.9564	0.0436	0.0456
20	0.9150	0.0850	0.0929
30	0.8757	0.1243	0.1419
45	0.8205	0.1795	0.2188
60	0.7693	0.2307	0.2999

TABLE B6: CH_4 Loading in decane at 328.15K (SRK-EOS)

P(bar)	$nC_{10}H_{22}$	nCH_4	CH_4 Loading
10	0.9581	0.0419	0.0438
20	0.9181	0.0819	0.0892
30	0.8801	0.1199	0.1362
45	0.8265	0.1735	0.2100
60	0.7766	0.2234	0.2877

APPENDIX C: Henry's constant for CO_2 and CH_4

TABLE C1: Henry's constant of CO_2 in decane at 308.15K

P (bar)	Mole of CO_2 in $C_{10}H_{22}$ (Kmol/hr)	Volume $C_{10}H_{22}$ (L/hr)	Concentration of CO_2 in $C_{10}H_{22}$ (mol/L)	Henry's constant (bar.L/mole)
10	1.3607	2000	0.6804	14.6983
20	3.0033	2000	1.5017	13.3186
30	4.9833	2000	2.4916	12.0403
45	8.8064	2000	4.4032	10.2198
60	14.3615	2000	7.1808	8.3557

TABLE C2: Henry's constant of CO_2 in decane at 318.15K

P (bar)	Mole of CO_2 in $C_{10}H_{22}$ (Kmol/hr)	Volume $C_{10}H_{22}$ (L/hr)	Concentration of CO_2 in $C_{10}H_{22}$ (mol/L)	Henry's constant (bar.L/mole)
10	1.1981	2000	0.5990	16.6934
20	2.6076	2000	1.3038	15.3401
30	4.2588	2000	2.1294	14.0885
45	7.3090	2000	3.6545	12.3136
60	11.3505	2000	5.6753	10.5722

TABLE C3: Henry's constant of CO_2 in decane at 328.15K

P (bar)	Mole of CO_2 in $C_{10}H_{22}$ (Kmol/hr)	Volume $C_{10}H_{22}$ (L/hr)	Concentration of CO_2 in $C_{10}H_{22}$ (mol/L)	Henry's constant (bar.L/mole)
10	1.0699	2000	0.5350	18.6930
20	2.3030	2000	1.1515	17.3686
30	3.7192	2000	1.8596	16.1325
45	6.2564	2000	3.1282	14.3852
60	9.4478	2000	4.7239	12.7013

TABLE C4: Henry's constant of CH_4 in decane at 308.15K

P (bar)	Mole of CO_2 in $C_{10}H_{22}$ (Kmol/hr)	Volume $C_{10}H_{22}$ (L/hr)	Concentration of CO_2 in $C_{10}H_{22}$ (mol/L)	Henry's constant (bar.L/mole)
10	0.4967	2000	0.2483	40.2698
20	1.0127	2000	0.5064	39.4979
30	1.5487	2000	0.7743	38.7429
45	2.3883	2000	1.1941	37.6844
60	3.2714	2000	1.6357	36.6813

TABLE C5: Henry's constant of CH_4 in decane at 318.15K

P (bar)	Mole of CO_2 in $C_{10}H_{22}$ (Kmol/hr)	Volume $C_{10}H_{22}$ (L/hr)	Concentration of CO_2 in $C_{10}H_{22}$ (mol/L)	Henry's constant (bar.L/mole)
10	0.4704	2000	0.2352	42.5206
20	0.9607	2000	0.4803	41.6364
30	1.4698	2000	0.7349	40.8205
45	2.2647	2000	1.1324	39.7399
60	3.1015	2000	1.5507	38.6912

TABLE C6: Henry's constant of CH_4 in decane at 328.15K

P (bar)	Mole of CO_2 in $C_{10}H_{22}$ (Kmol/hr)	Volume $C_{10}H_{22}$ (L/hr)	Concentration of CO_2 in $C_{10}H_{22}$ (mol/L)	Henry's constant (bar.L/mole)
10	0.4482	2000	0.2241	44.6265
20	0.9168	2000	0.4584	43.6290
30	1.4015	2000	0.7007	42.8126
45	2.1606	2000	1.0803	41.6555
60	2.9568	2000	1.4784	40.5844

APPENDIX D

D1: HYSYS RESULTS – Peng Robinson (PR-EOS)

Temperature	308.15K						318.15K						328.15K					
Composition CO2:CH4	1:0																	
	Liquid Fraction			Gas Fraction			Liquid Fraction			Gas Fraction			Liquid Fraction			Gas Fraction		
Pressure (bar)	CO2	CH4	n-Decane	CO2	CH4	n-Decane	CO2	CH4	n-Decane	CO2	CH4	n-Decane	CO2	CH4	n-Decane	CO2	CH4	n-Decane
10	0.1162	0.0000	0.8838	0.9994	0.0000	0.0006	0.1040	0.0000	0.8960	0.9990	0.0000	0.0010	0.0941	0.0000	0.9059	0.9983	0.0000	0.0017
20	0.2248	0.0000	0.7752	0.9996	0.0000	0.0004	0.2012	0.0000	0.7988	0.9993	0.0000	0.0007	0.1822	0.0000	0.8178	0.9988	0.0000	0.0012
30	0.3272	0.0000	0.6728	0.9996	0.0000	0.0004	0.2925	0.0000	0.7075	0.9993	0.0000	0.0007	0.2649	0.0000	0.7351	0.9989	0.0000	0.0011
45	0.4727	0.0000	0.5273	0.9994	0.0000	0.0006	0.4203	0.0000	0.5797	0.9991	0.0000	0.0009	0.3801	0.0000	0.6199	0.9987	0.0000	0.0013
60	0.6177	0.0000	0.3823	0.9990	0.0000	0.0010	0.5405	0.0000	0.4595	0.9987	0.0000	0.0013	0.4865	0.0000	0.5135	0.9982	0.0000	0.0018
Composition CO2:CH4	0.75:0.25																	
	Liquid Fraction			Gas Fraction			Liquid Fraction			Gas Fraction			Liquid Fraction			Gas Fraction		
Pressure (bar)	CO2	CH4	n-Decane	CO2	CH4	n-Decane	CO2	CH4	n-Decane	CO2	CH4	n-Decane	CO2	CH4	n-Decane	CO2	CH4	n-Decane
10	0.0861	0.0119	0.9020	0.7458	0.2536	0.0006	0.0772	0.0113	0.9115	0.7461	0.2529	0.0010	0.0700	0.0108	0.9192	0.7460	0.2523	0.0017
20	0.1644	0.0238	0.8118	0.7418	0.2578	0.0004	0.1478	0.0226	0.8296	0.7429	0.2564	0.0007	0.1343	0.0215	0.8442	0.7435	0.2553	0.0012
30	0.2351	0.0360	0.7289	0.7372	0.2624	0.0004	0.2120	0.0340	0.7540	0.7392	0.2602	0.0006	0.1932	0.0323	0.7745	0.7405	0.2584	0.0011
45	0.3279	0.0549	0.6172	0.7292	0.2703	0.0005	0.2971	0.0515	0.6514	0.7329	0.2663	0.0008	0.2720	0.0487	0.6793	0.7355	0.2633	0.0012
60	0.4053	0.0753	0.5194	0.7200	0.2793	0.0007	0.3695	0.0698	0.5607	0.7260	0.2730	0.0010	0.3400	0.0656	0.5944	0.7300	0.2685	0.0015
Composition CO2:CH4	0.5:0.5																	
	Liquid Fraction			Gas Fraction			Liquid Fraction			Gas Fraction			Liquid Fraction			Gas Fraction		
Pressure (bar)	CO2	CH4	n-Decane	CO2	CH4	n-Decane	CO2	CH4	n-Decane	CO2	CH4	n-Decane	CO2	CH4	n-Decane	CO2	CH4	n-Decane
10	0.0570	0.0234	0.9196	0.4958	0.5036	0.0006	0.0512	0.0223	0.9265	0.4962	0.5028	0.0010	0.0464	0.0213	0.9322	0.4963	0.5020	0.0017
20	0.1080	0.0463	0.8457	0.4918	0.5078	0.0004	0.0973	0.0440	0.8587	0.4929	0.5064	0.0007	0.0886	0.0421	0.8692	0.4936	0.5052	0.0012
30	0.1533	0.0686	0.7781	0.4876	0.5120	0.0004	0.1388	0.0653	0.7959	0.4894	0.5099	0.0007	0.1268	0.0625	0.8107	0.4907	0.5082	0.0010
45	0.2113	0.1014	0.6873	0.4811	0.5184	0.0005	0.1927	0.0963	0.7110	0.4841	0.5152	0.0007	0.1772	0.0921	0.7307	0.4862	0.5127	0.0011
60	0.2586	0.1333	0.6081	0.4746	0.5248	0.0006	0.2376	0.1276	0.6348	0.4787	0.5204	0.0009	0.2200	0.1209	0.6591	0.4817	0.5170	0.0013

D2: HYSYS RESULTS – Peng Robinson (PR-EOS) cont…

Temperature	308.15K						318.15K						328.15K					
Composition CO2:CH4	0.25:0.75																	
	Liquid Fraction			Gas Fraction			Liquid Fraction			Gas Fraction			Liquid Fraction			Gas Fraction		
Pressure (bar)	CO2	CH4	n-Decane	CO2	CH4	n-Decane	CO2	CH4	n-Decane	CO2	CH4	n-Decane	CO2	CH4	n-Decane	CO2	CH4	n-Decane
10	0.0284	0.0348	0.9368	0.2477	0.7518	0.0005	0.0255	0.0332	0.9413	0.2479	0.7511	0.0010	0.0232	0.0318	0.9451	0.2480	0.7503	0.0017
20	0.0537	0.0681	0.8782	0.2455	0.7541	0.0004	0.0484	0.0649	0.8867	0.2461	0.7532	0.0007	0.0441	0.0623	0.8936	0.2465	0.7524	0.0011
30	0.0760	0.0999	0.8241	0.2434	0.7562	0.0004	0.0689	0.0953	0.8358	0.2443	0.7551	0.0006	0.0631	0.0915	0.8454	0.2450	0.7540	0.0010
45	0.1045	0.1450	0.7505	0.2403	0.7593	0.0004	0.0955	0.1386	0.7659	0.2416	0.7577	0.0007	0.0880	0.1333	0.7787	0.2427	0.7563	0.0010
60	0.1278	0.1872	0.6850	0.2374	0.7621	0.0005	0.1177	0.1793	0.7030	0.2391	0.7601	0.0008	0.1091	0.1727	0.7182	0.2405	0.7583	0.0012

Composition CO2:CH4	0:1																	
	Liquid Fraction			Gas Fraction			Liquid Fraction			Gas Fraction			Liquid Fraction			Gas Fraction		
Pressure (bar)	CO2	CH4	n-Decane	CO2	CH4	n-Decane	CO2	CH4	n-Decane	CO2	CH4	n-Decane	CO2	CH4	n-Decane	CO2	CH4	n-Decane
10	0.0000	0.0462	0.9538	0.0000	0.9994	0.0006	0.0000	0.0440	0.9560	0.0000	0.9990	0.0010	0.0000	0.0422	0.9578	0.0000	0.9983	0.0017
20	0.0000	0.0897	0.9103	0.0000	0.9996	0.0004	0.0000	0.0857	0.9143	0.0000	0.9993	0.0007	0.0000	0.0823	0.9177	0.0000	0.9989	0.0011
30	0.0000	0.1308	0.8692	0.0000	0.9996	0.0004	0.0000	0.1252	0.8748	0.0000	0.9994	0.0006	0.0000	0.1204	0.8796	0.0000	0.9990	0.0010
45	0.0000	0.1882	0.8118	0.0000	0.9996	0.0004	0.0000	0.1806	0.8194	0.0000	0.9994	0.0006	0.0000	0.1741	0.8259	0.0000	0.9990	0.0010
60	0.0000	0.2409	0.7591	0.0000	0.9995	0.0005	0.0000	0.2318	0.7682	0.0000	0.9993	0.0007	0.0000	0.2240	0.7760	0.0000	0.9989	0.0011

D3: HYSYS RESULTS – Soave-Redlich Kwong (SRK-EOS)

Temperature	308.15K						318.15K						328.15K					
Composition CO2:CH4																		
	Liquid Fraction			Gas Fraction			Liquid Fraction			Gas Fraction			Liquid Fraction			Gas Fraction		
Pressure (bar)	CO2	CH4	n-Decane	CO2	CH4	n-Decane	CO2	CH4	n-Decane	CO2	CH4	n-Decane	CO2	CH4	n-Decane	CO2	CH4	n-Decane
10	0.1131	0.0000	0.8869	0.9995	0.0000	0.0005	0.1017	0.0000	0.8983	0.9991	0.0000	0.0009	0.0924	0.0000	0.9076	0.9985	0.0000	0.0015
20	0.2191	0.0000	0.7809	0.9996	0.0000	0.0004	0.1970	0.0000	0.8030	0.9994	0.0000	0.0006	0.1791	0.0000	0.8209	0.9990	0.0000	0.0010
30	0.3192	0.0000	0.6808	0.9997	0.0000	0.0003	0.2866	0.0000	0.7134	0.9994	0.0000	0.0006	0.2606	0.0000	0.7394	0.9990	0.0000	0.0010
45	0.4616	0.0000	0.5384	0.9995	0.0000	0.0005	0.4123	0.0000	0.5877	0.9993	0.0000	0.0007	0.3743	0.0000	0.6257	0.9989	0.0000	0.0011
60	0.6022	0.0000	0.3978	0.9992	0.0000	0.0008	0.5304	0.0000	0.4696	0.9989	0.0000	0.0011	0.4795	0.0000	0.5205	0.9985	0.0000	0.0015
Composition CO2:CH4																		
	Liquid Fraction			Gas Fraction			Liquid Fraction			Gas Fraction			Liquid Fraction			Gas Fraction		
Pressure (bar)	CO2	CH4	n-Decane	CO2	CH4	n-Decane	CO2	CH4	n-Decane	CO2	CH4	n-Decane	CO2	CH4	n-Decane	CO2	CH4	n-Decane
10	0.0839	0.0117	0.9044	0.7460	0.2535	0.0005	0.0755	0.0112	0.9133	0.7463	0.2528	0.0009	0.0687	0.0107	0.9206	0.7462	0.2523	0.0015
20	0.1603	0.0235	0.8162	0.7422	0.2575	0.0003	0.1448	0.0224	0.8328	0.7432	0.2562	0.0006	0.1321	0.0214	0.8465	0.7438	0.2552	0.0010
30	0.2298	0.0355	0.7347	0.7377	0.2619	0.0004	0.2080	0.0337	0.7583	0.7396	0.2598	0.0006	0.1902	0.0321	0.7777	0.7409	0.2582	0.0009
45	0.3213	0.0543	0.6244	0.7302	0.2694	0.0004	0.2921	0.0510	0.6569	0.7302	0.2694	0.0004	0.2682	0.0484	0.6833	0.7360	0.2630	0.0010
60	0.3981	0.0743	0.5276	0.7215	0.2779	0.0006	0.3640	0.0691	0.5669	0.7270	0.2721	0.0009	0.3359	0.0652	0.5989	0.7307	0.2680	0.0012
Composition CO2:CH4																		
	Liquid Fraction			Gas Fraction			Liquid Fraction			Gas Fraction			Liquid Fraction			Gas Fraction		
Pressure (bar)	CO2	CH4	n-Decane	CO2	CH4	n-Decane	CO2	CH4	n-Decane	CO2	CH4	n-Decane	CO2	CH4	n-Decane	CO2	CH4	n-Decane
10	0.0555	0.0231	0.9214	0.4960	0.5035	0.0005	0.0501	0.0221	0.9278	0.4963	0.5028	0.0009	0.0456	0.0212	0.9332	0.4965	0.5020	0.0015
20	0.1054	0.0457	0.8489	0.4921	0.5075	0.0004	0.0954	0.0436	0.8610	0.4932	0.5062	0.0006	0.0872	0.0419	0.8709	0.4939	0.5051	0.0010
30	0.1499	0.0679	0.7822	0.4881	0.5116	0.0003	0.1362	0.0647	0.7991	0.4898	0.5097	0.0005	0.1249	0.0621	0.8130	0.4910	0.5081	0.0009
45	0.2072	0.1004	0.6924	0.4819	0.5177	0.0004	0.1895	0.0956	0.7149	0.4846	0.5148	0.0006	0.1748	0.0917	0.7335	0.4867	0.5124	0.0009
60	0.2542	0.1322	0.6136	0.4756	0.5239	0.0005	0.2342	0.1257	0.6401	0.4794	0.5198	0.0008	0.2174	0.1204	0.6621	0.4822	0.5167	0.0011

Temperature	308.15K						318.15K						328.15K					
Composition CO2:CH4																		
	Liquid Fraction			Gas Fraction			Liquid Fraction			Gas Fraction			Liquid Fraction			Gas Fraction		
Pressure (bar)	CO2	CH4	n-Decane	CO2	CH4	n-Decane	CO2	CH4	n-Decane	CO2	CH4	n-Decane	CO2	CH4	n-Decane	CO2	CH4	n-Decane
10	0.0277	0.0344	0.9379	0.2478	0.7518	0.0004	0.0250	0.0329	0.9421	0.2480	0.7512	0.0008	0.0228	0.0316	0.9457	0.2481	0.7505	0.0015
20	0.0524	0.0673	0.8803	0.2457	0.7540	0.0003	0.0478	0.0646	0.8876	0.2462	0.7532	0.0006	0.0434	0.0619	0.8946	0.2466	0.7524	0.0010
30	0.0743	0.0988	0.8269	0.2437	0.7560	0.0003	0.0676	0.0946	0.8378	0.2445	0.7550	0.0005	0.0621	0.0911	0.8468	0.2451	0.7540	0.0009
45	0.1024	0.1437	0.7539	0.2407	0.7590	0.0003	0.0939	0.1378	0.7683	0.2419	0.7575	0.0006	0.0868	0.1328	0.7804	0.2429	0.7562	0.0009
60	0.1256	0.1858	0.6886	0.2378	0.7617	0.0005	0.1159	0.1784	0.7057	0.2395	0.7599	0.0006	0.1078	0.1722	0.7200	0.2407	0.7583	0.0010

D4: HYSYS RESULTS – Soave-Redlich Kwong (SRK-EOS) Continued:

Temperature	308.15K						318.15K						328.15K					
Composition CO2:CH4																		
	Liquid Fraction			Gas Fraction			Liquid Fraction			Gas Fraction			Liquid Fraction			Gas Fraction		
Pressure (bar)	CO2	CH4	n-Decane	CO2	CH4	n-Decane	CO2	CH4	n-Decane	CO2	CH4	n-Decane	CO2	CH4	n-Decane	CO2	CH4	n-Decane
10	0.0277	0.0344	0.9379	0.2478	0.7518	0.0004	0.0250	0.0329	0.9421	0.2480	0.7512	0.0008	0.0228	0.0316	0.9457	0.2481	0.7505	0.0015
20	0.0524	0.0673	0.8803	0.2457	0.7540	0.0003	0.0478	0.0646	0.8876	0.2462	0.7532	0.0006	0.0434	0.0619	0.8946	0.2466	0.7524	0.0010
30	0.0743	0.0988	0.8269	0.2437	0.7560	0.0003	0.0676	0.0946	0.8378	0.2445	0.7550	0.0005	0.0621	0.0911	0.8468	0.2451	0.7540	0.0009
45	0.1024	0.1437	0.7539	0.2407	0.7590	0.0003	0.0939	0.1378	0.7683	0.2419	0.7575	0.0006	0.0868	0.1328	0.7804	0.2429	0.7562	0.0009
60	0.1256	0.1858	0.6886	0.2378	0.7617	0.0005	0.1159	0.1784	0.7057	0.2395	0.7599	0.0006	0.1078	0.1722	0.7200	0.2407	0.7583	0.0010
Composition CO2:CH4																		
	Liquid Fraction			Gas Fraction			Liquid Fraction			Gas Fraction			Liquid Fraction			Gas Fraction		
Pressure (bar)	CO2	CH4	n-Decane	CO2	CH4	n-Decane	CO2	CH4	n-Decane	CO2	CH4	n-Decane	CO2	CH4	n-Decane	CO2	CH4	n-Decane
10	0.0000	0.0456	0.9544	0.0000	0.9995	0.0005	0.0000	0.0436	0.9564	0.0000	0.9992	0.0008	0.0000	0.0419	0.9581	0.0000	0.9985	0.0015
20	0.0000	0.0887	0.9113	0.0000	0.9997	0.0003	0.0000	0.0850	0.9150	0.0000	0.9994	0.0006	0.0000	0.0819	0.9181	0.0000	0.9990	0.0010
30	0.0000	0.1295	0.8705	0.0000	0.9997	0.0003	0.0000	0.1243	0.8757	0.0000	0.9995	0.0005	0.0000	0.1199	0.8801	0.0000	0.9992	0.0008
45	0.0000	0.1866	0.8134	0.0000	0.9997	0.0003	0.0000	0.1795	0.8205	0.0000	0.9995	0.0005	0.0000	0.1735	0.8265	0.0000	0.9992	0.0008
60	0.0000	0.2392	0.7608	0.0000	0.9996	0.0004	0.0000	0.2307	0.7693	0.0000	0.9994	0.0006	0.0000	0.2234	0.7766	0.0000	0.9991	0.0009